Designed Multiple Ligand Approach: Design, synthesis, and evaluation of anticancer Potential of novel PARP1 and STAT3 as Dual Inhibitor

Submitted in partial fulfillment of the requirements for the award of

Bachelor of Pharmacy

Submitted by

N. BACEER (39050008)

S. DILIP KUMAR (39050013)

V.KARTHIK (39050022)

M.KATHIRESAN (39050023)

R. VELMURUGAN (39050058)

SCHOOL OF PHARMACY

SATHYABAMA INSTITUTE OF SCIENCE & TECHNOLOGY

(Institution Deemed to be University-U/s 3 of the UGC Act, 1956)

Rajiv Gandhi Salai, CHENNAI – 600119

May,2023

SATHYABAMA
INSTITUTE OF SCIENCE AND TECHNOLOGY
(DEEMED TO BE UNIVERSITY)
Accredited "A" Grade by NAAC | 12B Status by UGC | Approved by AICTE
www.sathyabama.ac.in

Dr. Kaviarasan L., M.Pharm., Ph.D.,

Associate Professor

BONAFIDE CERTIFICATE

This is to certify that the thesis entitled **"Designed Multiple Ligand Approach: Design, synthesis and evaluation of anticancer Potential of novel PARP1 and STAT3 as Dual Inhibitor"**, submitted by

N. BACEER (39050008)

S. DILIP KUMAR (39050013)

V.KARTHIK (39050022)

M.KATHIRESAN (39050023)

R. VELMURUGAN (39050058)

to the **SATHYABAMA INSTITUTE OF SCIENCE & TECHNOLOGY, chennai-600119** for the award of the degree of **Bachelor of Pharmacy** by Research is a bona-fide record of research work carried out by him/her under my supervision. The contents of this thesis, in full or in parts, have not been submitted to any other Institute or University for the award of any degree, diploma, associateship, fellowship or any similar title and that it represents entirely an independent work on the part of the candidate.

Chennai-600119

Date: 15/04/2023

Research Guide

Dr. Kaviarasan L., M.Pharm., Ph.D.,

Associate Professor

SATHYABAMA SCHOOL OF PHARMACY Chennai 600 119.

Approved by Dean

Dr. P. Shanmugapandiyan

DEAN
SCHOOL OF PHARMACY
SATHYABAMA
INSTITUTE OF SCIENCE AND TECHNOLOGY
(DEEMED TO BE UNIVERSITY)
Jeppiaar Nagar, Rajiv Gandhi Salai
Chennai 600 119.

Authenticated by Examiners

1. 15/04/23

2.

DECLARATION

I do hereby declare that the work presented in the thesis entitled **"Designed Multiple Ligand Approach: Design, synthesis and evaluation of anticancer Potential of novel PARP1 and STAT3 as Dual Inhibitor"**, submitted by me to the **SATHYABAMA INSTITUTE OF SCIENCE & TECHNOLOGY**, Chennai-600119 for the award of the degree of **Bachelor of Pharmacy (2019-2023)** by Research is an original record of research work carried out by me under the supervision of **"Dr. Kaviarasan L M.Pharm., Ph.D.,, Associate Professor, Department of Pharmacy".** The contents of this dissertation, in full or in parts, have not been submitted to any other Institute or University for the award of any degree or diploma, membership, fellowship, associateship etc... In keeping with the general practice in reporting scientific observation, due acknowledgement has been made whenever the work described is based on the findings of other investigators.

Place Chennai
Date: 15/04/2023

N. Bacer
N. BACEER (39050008)

S. DILIP KUMAR (39050013)

J. Karthik
V.KARTHIK (39050022)

M. Kathi
M.KATHIRESAN (39050023)

R. VELMURUGAN (39050058)

ABSTRACT

Introduction

Dual or multi-targeting of cancer proteins by a single compound shows an efficient, logical and alternative approach for a combination of drugs. Blockage of more than one oncoprotein or pathway is now a standard approach in modern cancer therapy. Multiple inhibition is typically achieved with two or more drugs which is achieved by DML approaches. Inhibition of numerous oncoproteins or pathways is currently a common strategy in cancer treatment. in this study that single agents inhibiting both PARP1 and STAT3 at the same time may cause substantial synergistic mortality in cancer cells.

Objective

The objective of the study was to synthesize a series quinazolinone derivatives and evaluate their possible ***in vitro*** anticancer activity.

Methods

Herein, we designed the title compounds based on SAR of known inhibitors of both PARP1 and STAT3 by DML approach. The synthetic scheme, which was followed for the preparation of a series of 60 title compounds outlined in scheme 1. The purity of the synthesized compounds was ensured by various spectral analyses. Docking studies of designed molecules were performed using Schrödinger suite. The compounds were tested for their in vitro cytotoxic potential using MDA-MD-231 cells.

Results

In *in silico* molecular docking studies, the compounds show better binding affinity like known PARP1 and STAT3 inhibitors. All the 10 synthesized compounds were subjected to an *in-vitro* cytotoxicity study by MTT assay method with cell line MDA-MB-231 cell line. All the tested compounds displayed an IC_{50}> 115 µg/mL at a concentration range of 30–250 µg/mL. The cellular evaluation indicates that the anticancer profile of compounds 1f are significant when compared to the standard drug (Olaparib and niclosamide) against MDA-MB-231

Conclusion

The present course of work revealed that among the synthesized derivatives, compound 1f substituted with chloro benzene possess the significant activity. From the present investigation, it may be concluded that quinazolinone benzamide derivativesneedtoundergofurtherinvestigationstodevelop as a potential candidate drugfor cancer.

Keywords

PARP1,STAT3**,** Schrodinger software, anticancer activity, MDA-MB-231, *in silico* ADMET.

LIST OF TABLES

LISTS OF FIGURES

LISTS ABBREVIATION

1	SAR	Structural Activity Relationship
2	PARP	Poly (ADB) ribose polymerization
3	STAT3	Signal transducer and activator of transcription 3
4	DML	Designed Multiple ligand approaches
5	NMR	Nuclear Magnetic Resonance
6	MS	Mass spectra
7	IR	Infra-red spectra
8	MTT	(3-(4, 5-dimethylthiazolyl-2)-2, 5-diphenyltetrazolium bromide)
9	DMBA	7,12-Dimethylbenz[a]anthracene
10	OECD	Organization for Economic Co-operation and Development
11	ADMET	Absorption, Distribution, Metabolism, Elimination, Toxicity
12	FDA	Food and Drug Administration
13	DNA	Deoxyribonucleic Acid
14	BRCA	breast cancer
15	DSB	Double-Strand Break
16	NER	Nucleotide Excision Repair
17	MMR	Mismatch Repair
18	HR	Homologous Recombinational Repair
19	PDB	Protein data bank

1.INTRODUCTION

1.1. CANCER

Cancer has emerged to become a dreadful threat affecting human beingsglobally.Amongvariousdiseases,cancerhasbecomeabigthreattohumanbeingsglobally (1). Cancer, also known as a malignant tumor or malignant neoplasm, is agroup of diseases involving abnormal cell growth with the potential to invade orspread to other parts of the body. Not all tumors are cancerous; benign tumors donot spread to other parts of the body. Cancer results from a series of molecularevents that alter the fundamental properties of cells (2). In cancer cells, the normalcontrol systems that prevent cell overgrowth and the invasion of other tissues aredisabled. These altered cells proliferate and grow in the presence of signals thatnormally inhibit cell growth. These cells no longer require special signals to inducecell growth and division. Eventually, they develop new characteristics, includingaltered cell structure, decreased cell adhesion, and production of new enzymes.These heritable changes allow the cell and its progeny to divide and grow, even inthe presence of normal cells that typically inhibit the growth of nearby cells. Suchchangesallowthecancer cellsto spreadandinvadeother tissues(3,4).

1.2. DESIGNEDMULTIPLELIGANDAPPROACHES(DML)

With this approach, once the potency ratio is determined is it fixed within themolecule hence the variable pharmacokinetics usually seen with combinations oftwo single agents will not affect the potency ratio of a DML in the same way.However,itshouldbenotedthatDMLsarejustassusceptibletometabolismasanyotherdrug,reducingoreliminatingthebiologicalactivityorpharmacodynamicprofileof the compound. Being single molecules DMLs will not suffer from drug-druginteractions unless combined with another drug. There is also an opportunity forstructuralnovelty–thedesignofaDMLisnotjustamatterofjoiningtwopharmacophores together, it is a creative process to balance multiple SARs whilemaintaining drug-like properties. Development costs for a DML are likely to besignificantly lower than the development of a multiple drug combination, but thismustbebalancedwithotherpotentialdownsidessuchasmolecularweightinflation,thechallengeofbalancingmultipleSARsandpotentiallymorechallengingsynthesisareallp

resentdangers(5,6).

In this work, we focus on DMLs that target two different classes of theenzyme, rather than two enzymes performing the same type of transformation.Deliberate strategies to adopt such a DML approach at the outset for enzymeinhibitors in cancer are not commonly reported. Recent progress has been mostsuccessfulincombiningthehistonedeacetylase(HDAC)pharmacophorewithothe renzymeinhibitoractivities,suchaskinases.Examplesofsuccessfulkinase-HDAC,DMLs have now reached the clinic in oncology pioneered by Curis, although noneare yet approved by the Food and Drug Administration (FDA) (7). Inspired by thisprogress we have been focused on designed combinations of Poly (ADP-ribose)polymerase1(PARP1)andSignaltransducerandactivatoroftranscription3(STAT3)inhibitorsin cancer study.

1.3. POLY(ADP-RIBOSE)POLYMERASE1

PARP1 is a family of enzymes discovered in 1963 by Chambon and its co-workers, which shares the ability to catalyze the transfer of ADB ribose to targetprotein(8).Thisfamilyofenzymesplaysacrucialroleinvariouscellularprocessess uch as transcription, modulation of chromatin structure, replication, recombinationandDNArepairs.Thereare18membersofthePARPenzymeencodedtilln ow(9).Amongthem,PARP1isbestknownforitsinvolvementinDNArepair,cellproliferatio nandcelldeath.ThepharmacologicalinhibitionofPARPhasthepotentialtoenhancethec ytotoxicityofcertainDNAdamagingofanti-cancerdrugs,reduce cell necrosis, down-regulate the multiple pathways in inflammatory andinjured tissues. Literature has shown that PARP1 action is low in a maximum ofnormalhuman cells, whereas itis significantly upregulated in several primarycancerousdiseaseslikelymphomasandcancerofthebreast,uterusandovary(10).Hence, nowadays the understanding of the function and importance of the PARP1enzyme has been increased due to its vital role in DNA repair, among other things,leading to investigations of specific inhibitors in the drug development process invarious pathological conditions including cancer, a neurodegenerative disorder,metabolicdisorder andvarious disorders (11).

1.3.1. STRUCTURE,FUNCTIONANDREGULATIONOFPARP1

PARP1 is the first protein in the family identified and the major enzyme tohave poly ADP ribosylation activity inside the cell as well as major DNA

damage.PARP1 is the most active isoform accounting for more than 90% of its functions(12).ThePARP1enzymehasthreemainfunctionaldomains:thefirstoneistheN

terminalDNAbindingdomain(13).Itcontainstwomainzincfingermotifsandbindstobothsingleaswellasdouble-strandedbreaks.Recently,thethirdzincfingerhasbeen identified and it is important for coupling damage induced changes in DNAdomains to alterations in PARP1 catalytic activity; the second domain is the centralmodificationdomain,whichcontainsBRCTdomains(BRCACarboxyTerminal)andother than this, it has two amino acid residue domains *i.e*. Glutamate and Lysineresidues which serve as an acceptor of ADP-ribose moiety and has protein-proteininteraction domain, which is present in other components of the DNA damageresponse pathways; the third domain is C terminal catalytic domain where NAD^+binds and acts as a substrate for PARP1 (14). **Figure 1** shows the structure of thePARP1enzyme.

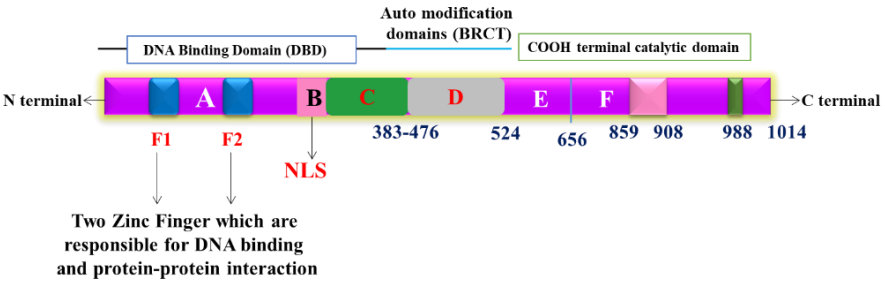

Figure1. StructureofPARP1enzyme.

When the PARP1 enzyme is activated by DNA damage, it cleaves NAD^+ forthe ADP-ribosylation of protein acceptors, generating nicotinamide as a by-productandfacilitatesDNArepair(15).Thelarge113kDanuclearproteinusuallyhasalowintrinsic enzymatic activity which may be significantly enhanced by binding bothsingle strands DNA breaks (SSDB) and double strands DNA breaks (DSDB) *via*either of its N-terminal zinc fingers, bringing about conformational changes throughits third zinc finger to increase catalytic activity at the C-terminal. As large amountsof negative charges are conferred by adding extensive polymers of ADP-ribose(PAR),PARP1modulatestheactivityofitssubstratesandcontrolsseveralimportant cellular functions such as DNA damage repair, transcriptional regulationand cell death (16). The studies reveal that the PARP1 has contributed to attaininggenomic integrity by increasing base excision repair in other anti-cancer treatedcells and also PARP1 contributes to genomic surveillance in interaction with othernick-sensor like DNA ligase III adaptor factors and components of BER complex(17).**Figure2**showsdifferentbiologicalfunctionsofthePARP1enzyme.Thethree-consequenceactivationofPARP1playsanimportantroleinthedrugdevelopment

process *i.e.,* i) role of DNA repair; ii) it can deplete cellular energetic pool, whichproduces cell dysfunction and necrosis; iii) promotes the transcription of the pro-inflammatorygene.VariousmodelstudieshaverevealedthatPARP1isinvolvedinmulti-processes,allofwhich is involvedin DNA relatedtransaction.

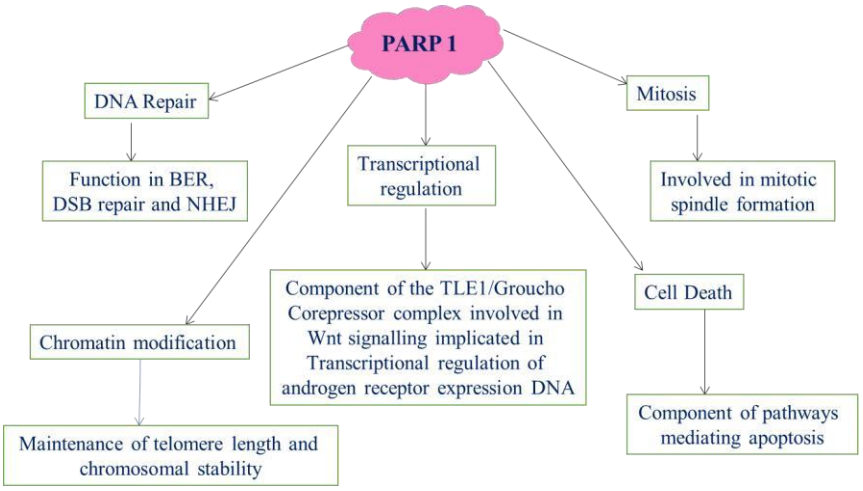

Figure2.ThedifferentbiologicalfunctionsofPARP1.

1.3.2. PARP1ANDCELLREPAIRPATHWAYS

ThehumancellhasfiveprimarypathwaysofDNArepair,whicharemediatedby PARP1. These include direct repair, mismatch repair (MMR), base excisionrepair (BER), nucleotide excision repair (NER) and double-strand break (DSB)recombinationalrepair(bothnon-homologousendsjoiningandhomologousrecombinational repair (HR) (17).Hence, targeting DNA repair pathways hasbecome an effective strategy for sensitizing cancer cells to the discovery of newchemotherapy agents. As targeting the DNA repair pathway of the PARP1 enzymeforcancertreatmentisthefocusofthiswork,manyliteraturesurveyshavedescribedthatthe PARP1 enzymeitselffollows manyDNA repairspathways**.**

1.3.3. PARP1ANDCELLDEATH

PARP1servesasasurvivalfactorinthepresenceoflow-levelDNAdamagebut in extensive or excessive DNA damage, it causes cell death due to over usageofNAD+.DuringexcessiveDNAdamage,PARP1hyperactivationleadstoextendedpoly (ADP ribose) synthesis and excessive consumption of NAD^+, which is

basedupon the cellular context. This intense PARP synthesis may induce cell death *via*necrosis or apoptosis (**Figure 3**). The main feature of apoptosis and necrosis is itsdependencyonATPforthedegradationofcellularstructure.Themodeofcelldeath

isdeterminedbytheintensityofDNAdamagingstimuli.Whetherapoptosisisproducedby mildstimuliandnecrosis isinitiatedby severeones(18).

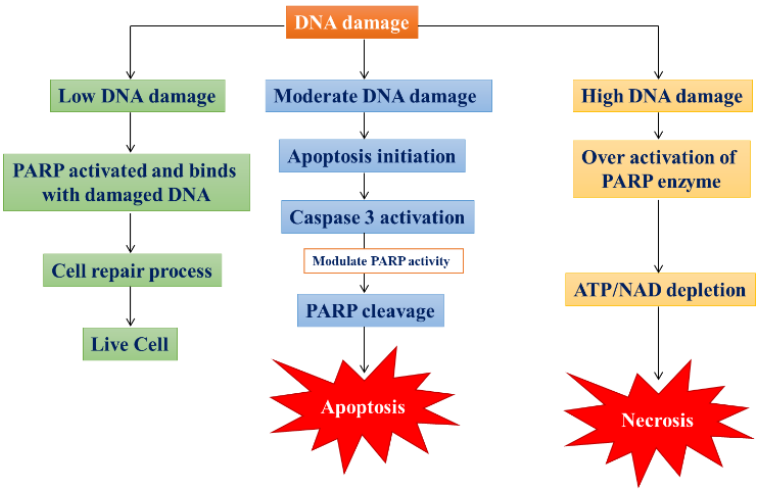

Figure 3.PARP1andcelldeath.

1.3.4. ROLEOFPARP-1INAPOPTOTICPATHWAYS

Apoptosisistheprocessofthebiochemicalrestrictedpathwayofprogrammed cell death or cell suicide. It is essential for proper homeostasis andsurvival in multi-cellular organisms (19). The apoptotic process needs ATP and isgenerally divided into three main phases *i.e.*, initiation, effectors and execution.Caspases are cysteine proteases that digest cellular proteins in the last phase ofapoptosis,inwhichthecellisrestructuredthroughtheformationofapoptoticbodies.Sev eralstudiesshowthatPARP1hyper-activationproducesenormousDNAdamageandisresponsiblefor80to90%lossoftheco enzymeNAD$^+$pool.ItisalsodemonstratedthatthelossofNAD$^+$precedestheinductionof mitochondrialdepolarization.Inaddition,themetabolicpathwaysrelyingonNAD$^+$availa bilitysuchas glycolysis, the TCA cycle and oxidative phosphorylation are chiefly impairedleading to a loss of ATP production and thereby amplifying the energetic depletionphenotype. This ATP depletion occurs first in the mitochondria and is followed by alossin boththecytosolandthe nucleus (20).

1.3.5. ROLEOFPARP-1INNECROTICPATHWAYS

Inhibition or absence of PARP-1 provides significant protection in diseasemodels like stroke myocardial infarction and ischemia which are characterized bynecrotic cell death. PARP over-activation during necrosis depletes the cell of NAD$^+$and ATP stores. It is also suggested that PARP over activation-induced necrosismayberelatedtointracellularacidificationbyH$^+$ionsformedasaby-

productof

NAD^+catabolism(34).WhenpolyADPribosylationproducedinlargequantitiescanmigratefromthenucleusintothecytosol,ittriggersthereleaseofthemitochondrialprotein Apoptosis-Inducing Factor (AIF), a flavoprotein which is transferred to thenucleus to condense with the chromatin, and thereby activates endonucleasesleadingtonecrosis (21).

1.3.6. PARP1INHIBITORS

PARP has been the center of attention of many medicinal chemists for over20yearsbutnowadays,theinterestinPARPinhibitorshasincreasedasPARPsareattractiveantitumordrugdiscoveringtargetsconsideringthatPARPinhibitioncouldsuppress DNA damage repair and sensitize tumor cells to DNA damage agents.ThedevelopmentofPARP1inhibitorshasprogressedtoagreatextentoverthelastfew years. Hence some of the PARP inhibitors have entered clinical development.PARP1inhibitionwhenconsideredatargetforoncology,actsasachemo-potentiator because most anticancer therapeutics focus on DNA damage as a tooltoeradicatetheexpeditiouslysplittingcancercells.DNArepairforabundantcancerouscelltypesiscarriedoutbythePARP1mediatedrepairpathway.Therefore,theinhibitionofPARP1alongwithDNAdamagingchemotherapeuticsorradiationisaverycompetenttooltojeopardizethecancercellDNArepairmechanism,ensuing genomicdysfunctionandcelldeath(22).

Breast Cancer linked genes BRCA1 and BRCA2 have been distinguishedhitherto as tumor suppressor genes that play an obligatory part in the repair ofdouble-strandbreaks(DSB)inDNA*via*aprocesscalledhomologousrecombination. Although PARP1 inhibition will contribute to an escalation in singlestrand breaks (SSB), these SSBs will ultimately lead to double-strand DNA breaks(DSB) through replication fork collapse. DSBs in the existence of HR lacking celltypes cause chromosomal aberrations and vulnerability of the genome resulting incelldeath.Thisincidentisreferredtoassyntheticlethality,specificallysincethelossof one gene function will result in cell susceptibility (*i.e*., the loss of PARP1 orBRCA1/2) but the loss of both is fatal (*i.e*., BRCA1/2 deficient cells and PARP1inhibitor). Some of the PARP1 inhibitors (**Figure 4**) have demonstrated promisingresults both as single agents in tumors with BRCAness exploiting the syntheticlethalityconceptorusedincombinationwithradiationorotherchemotherapydrugsexhibitingenhancedantitumor potencyin various cancers (23).

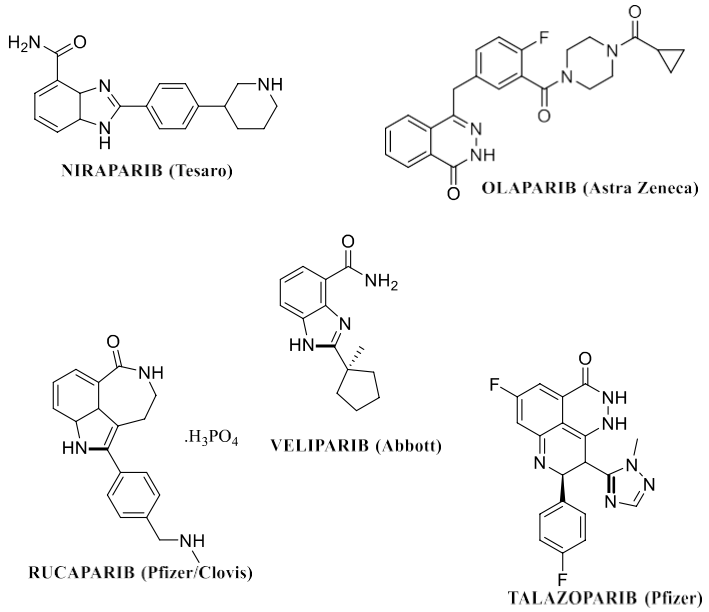

Figure 4.ChemicalstructureofPARP1inhibitors.

1.4. SIGNALTRANSDUCERANDACTIVATOROFTRANSCRIPTION3

STAT3isatranscriptionfactorthatisencodedbySTAT3anditisamemberofafamilyofsevenproteinsi.e.,STAT1,STAT2,STAT3,STAT4,STAT5aSTAT5b,STAT6. These proteins are known to play an important role in growth factor andcytokine signaling, which includes promoting cell development, differentiation andimmune responses. The STAT proteins are latent cytoplasm transcription factorsthattransfercytokinesandgrowthfactorsfromthecellmembranetothenucleustoregulate the gene expression from critical to normal cellular processes, includingdifferentiation, cell development, proliferation, survival, angiogenesis and immunefunction (23). All the 7 human STAT proteins range between 750-850 amino acidsandaresituatedonthreechromosomalclustersandSTAT3islocatedonchromosome 12 (47). Among seven STAT proteins, STAT3 genes are constantlyact it and commonly seen in a majority of human cancer cells and tumor tissuessuchasbreastcancer,melanoma,lungcancer,pancreaticcancer,prostatecancer,ovariancancer,leukemia’sandlymphomas.ThetargetofSTAT3activationinhibitsthetumorgrowthandmetastasisboth*invitro*and*invivo*withoutinfluencingnormalcells, thus signifying that STAT3 could be applicable as a molecular target formalignancytreatment (24).

1.4.1. STRUCTURE,FUNCTIONANDREGULATIONOFSTAT3

All the STAT family consists of 6 domains: NH2 terminal, coiled-coil domain,DNAbindingdomain, linker,SH2andCterminaltransactivationdomains(25).The functional domains of STAT3 enzyme comprise the dimerization domains andcoiled-coildomainsattheN-terminus,aSrcHomology(SH2)domain,whichinvolvestheinteractionoftwomonomersthroughphosphotyrosine705andformation of dimerization, DNA binding domains, transcription activation at the Cterminalend.Amongthesedomains,SH2domainsandtranscriptionactivationatCterminus end play a vital role in the activation of STAT3. STAT3 is activated by CTry705 and serine residue at 727. The SH2 region is a well-characterized smallproteinmodulethatcontainsabout100aminoacids.Itisresponsibleforthebindingof STAT3totyrosinephosphorylatedreceptorandalsohomodimerizationorheterodimerization of two STAT monomers necessary for DNA binding and alsogeneexpression.Duetothewidefunctionsofthesedomainsi.e.SH2region,NH2-terminalandDNA-bindingdomain,itwillbecomeanoveltargetforvariouspathologicalanddiseaseconditions(26).**Figure5**illustratesthestructureofSTAT3enzyme. The STAT3 protein is involved in several cellular functions (**Figure 6**). Itregulates genes that are involved in cell growth and division, cell movement andself-destructionofcells(apoptosis).TheSTAT3proteinisactiveintissuesthroughout the body. It plays a significant role in the development and function ofseveral body systems and is essential for life. In the immune system, the STAT3protein transmits signals for the maturation of immune system cells, especially Tcells and

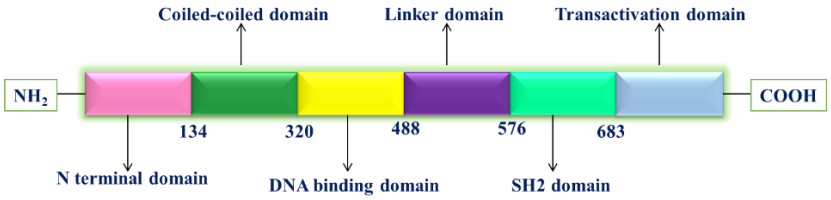

B cells. These cells help control the body's response to foreign invaderssuchasbacteria andfungi.

Figure 5.Structure ofSTAT3.

In addition, the protein is involved in the regulation of inflammation, due towhichtheimmunesystemrespondstoinfectionorinjury.Thesecellsarenecessaryfor the normal development and maintenance of bones (27). The nominated signaltransduction of STAT3 is initiated by the recruitment of STAT3 to macromoleculeactivated membrane receptor complication, which leads to key phosphorylation onTry705.Thisinturninducesaconfigurationalchangeresultingintail-to-taildimerizationmediatedprocessreciprocaltoSH2/Try705peptideligandinteractions.The activation of STAT3 protein is rapid, transient and regulates the nuclear genesthat control fundamental biological processes including cell proliferation, survivaland development. For example, Src, Janus Kinase and epidermal growth factorreceptor family tyrosine kinases are frequently activated in tumor cells and induceSTAT3 activation. STAT3 induces cell death and reduces the expression of anti-apoptic gene that encodes a member of BCL-2 family such as BCL-XL and MCL-L.STAT3canbephosphorylatedonaserineresiduenearthecarboxyend.However,STAT3hasavitalroleincellgrowthanditsactivationhasbeendescribedinnearly70% of solid and hematologic tumors; hence it provides good reason to search forspecificdirect inhibitors (29).

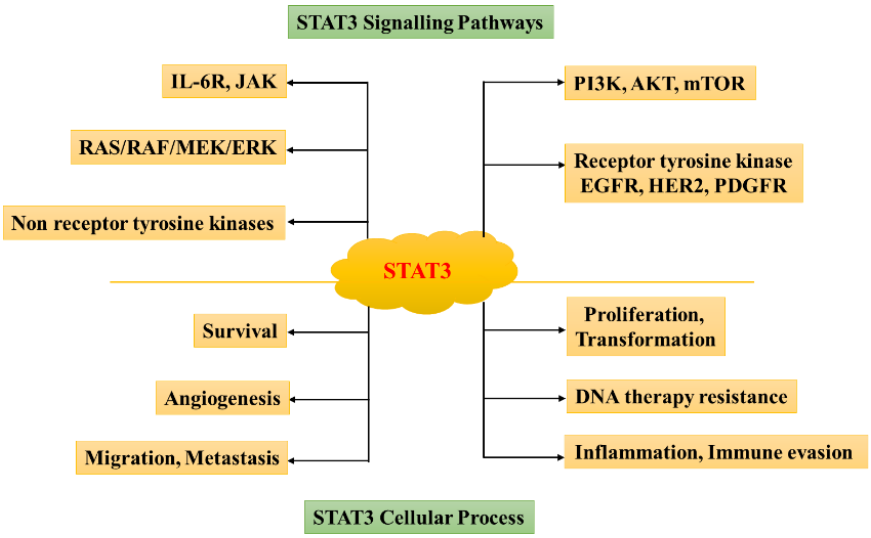

Figure6. CellularprocessesofSTAT3

1.4.2. STAT3ACTIVATIONINNORMALCONDITIONS

STAT3 activation in normal pathological conditions drives a well-organizedgene regulation schedule. After STAT3 is exposed to cytokine

stimulation, theproteincanreachamaximumofphosphorylationswithinthefirst15-60minutes,butSTAT3activationgraduallydecreasesinthefollowinghours.TheactivationprocessismediatedbytheJAKfamilyoftyrosine-kinases,mostnotablybyJAK1.STAT3 canbeactivatedindependentofJAKsbyothernonreceptortyrosinekinases,mostlybyc-Src kinases.

1.4.3. STAT3INAPOPTOSIS ANDCANCERCELLPROLIFERATION

Accumulating substantiation shows that continual activation of STAT3 isrequired for aberrant cell proliferation in carcinogenesis and also participates incellularproliferationandsurvival.BothcMycandcyclinD1arerequiredforregulationoftheG1phaseofthecellcycle(64).EvidenceindicatesthatconstitutiveSTAT3signalingisassociatedwithup-regulationofcyclinD1andcMycexpression,contributing to accelerated cell-cycle progression. STAT3 has also been shown toup-regulatetheexpressionofgrowthpromotinggenePIM-1.Consistentwithitsroleincellularproliferation,variousstudieshaveconfirmedthatSTAT3signalingprovides survival signals and suppresses apoptosis in cancerous cells. Theseeffects are mediated through the expression of Bcl2, BclxL, Mcl1, and cIAP2. Theapoptosisisregulatedbythetwopathwaysnamelyextrinsicandintrinsicpathways.The extrinsic pathway is initiated by ligands binding to the death receptor and itdirectly activates caspases to initiate the apoptosis program. The intrinsic pathwayis regulated at the mitochondria whereby the balance of pro-apoptotic (e.g., Bim,Bad, Bik, PUMA, and NOXA) and anti-apoptotic (e.g., Bcl-2, Bcl-xL, Mcl-1, A1, andBcl-w)proteinsfromtheBcl-2proteinfamilydeterminestheintegrityofthemitochondrialmembrane(30).

1.4.4. STAT3INANGIOGENESIS

Angiogenesis is an essential step in tumor development and metastasis.Vascular endothelial growth factor (VEGF) is the most intense angiogenic proteinsecreted from tumor cells that binds to the transmembrane receptor of endothelialcells and produces neovascularization. STAT3 has direct transcriptional activatorsofVEGFgene.TheconstitutiveactivationofSTAT3upregulatestheVEGFexpression and tumor angiogenesis in melanoma cells and additionally a fewinvestigations suggest that STAT3 activation regulates both VEGF expression andangiogenesisinhumanpancreaticcells.ButthetargetingofSTAT3inhibitionblocksb

oth VEGF and angiogenesis. A few investigations reported that STAT3 inducesexpressionofhypoxia-induciblefactor-1α(HIF1α),anotherkeymediatorofangiogenesis.Inhypoxicconditions,bothSTAT3and HIF1αbindsimultaneouslytotheVEGFpromotorleadingtoitsmaximumtranscriptionalactivationandangiogenesis(31).

1.4.5. STAT3ASTARGETFORCANCER

AmongalltheSTATproteinfamily,STAT3hasapivotalroleinthedevelopment of carcinogenesis, sinceit critically regulates thetranscription ofmultiplekeygenesinvolvedinmetastasis,immuneresponse,angiogenesis,apoptosis differentiationandcellproliferation.SincethediscoveryoftheassociationofconstitutiveSTAT3activationwithmalignanttransformation,supportingliteraturehas validated STAT3 as a cancer drug target as STAT3 is constitutively activatedduringdiseaseprogressionandmetastasisinavarietyofcancers.ImproperactivationofSTAT3hasbeenexposedtovarioustypesofsolidandhaematologicalcancers, however, blocking the STAT3 signaling pathway by various means iseffective in killing cancer cells in various animal experimental models. A number ofstudies reveal that STAT3 has been found to have an important role in maintainingcancer cell in both *in-vitro* and *in-vivo* models. **Figure 7** shows the schematicmechanismsofSTAT3contributingtocarcinogenesis.Duetoitsvitalroleincancerprogression, STAT3 is considered as a signaling molecule with anti-carcinogenicpropertiesand alsoconsideredashavinggoodanti-cancer activity(31).

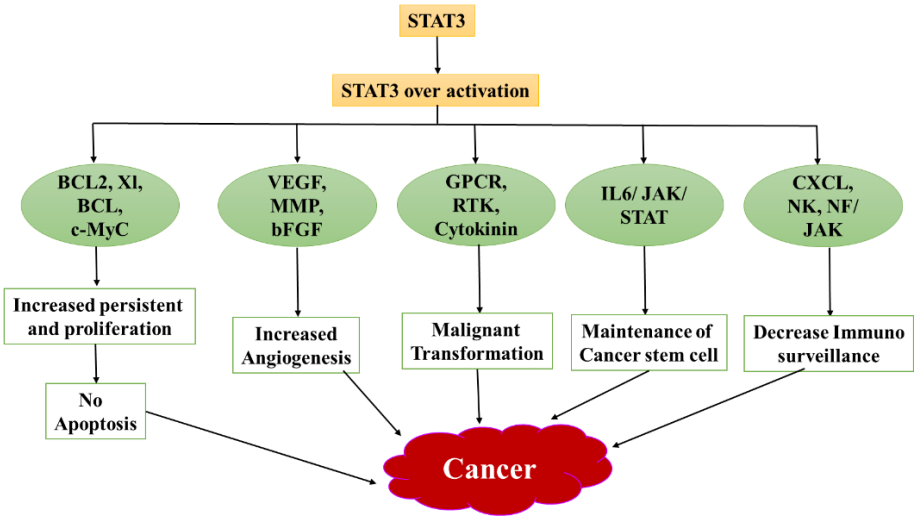

Figure7.contributionof**STAT3**tocarcinogenesis

1.4.6. INHIBITORSOFSTAT3

SeveralresearchgroupshavedevelopeddifferentsmallmoleculesasSTAT3inhibitorsasanapproachtowardsanticancertherapeutics.TheSTAT3initialhomodimerization is due to its transcriptionally active translocation to the nucleusand this process was initiated by phosphorylation of Try 705 at C terminal to theSH2 domain, which leads to dimerization through reciprocal SH2 phosphorylationinteraction(74).AmongvariousdomainsinSTAT3,SH2domainisthepri marytargetinthedesignofvarioussyntheticcompoundsaspotentanti-canceragentsaccordingtophosphotyrosineor phosphotyrosinemimetic(30).

1.4.7. STAT3:DIRECTINHIBITORS

A few STAT3 inhibitors (**Figure 8**) have been reported to date and notedherein,whichisareflectionoftheenhancedactivityinthisarenainrecentyears.Ofthese inhibitors, a few shows good activity in terms of the inhibition of STAT3biologicalfunctionsandtheassociatedantitumorcelleffects,aswellastheinhibitionoftumorgrowthinthemousemodels displaying humantumors. (27).

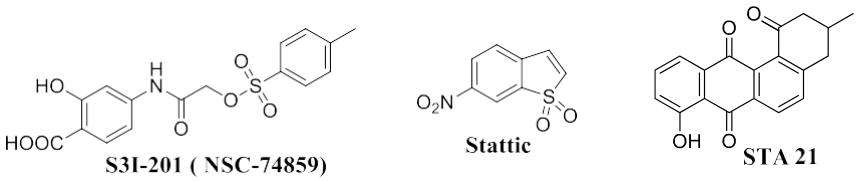

Figure8.ChemicalstructureofdirectSTAT3inhibitors.

1.4.8. STAT3INHIBITORFORSRCHOMOLOGY2 (SH2)DOMAIN

SH2 contains protein tyrosine phosphatase 2 which is encoded by PTPN11gene.Itiswidelyinvolvedintranscriptionalregulation,cellulardifferentiation,migration,cytokinesignalingandtumorcellproliferation.Thisgenethenundergoesgermlineorsomaticmutationandisreportedtoassociatewith NoonanandLEOPARD syndromes with tumor development of lung, breast, cervical cancer andskin. The elevated expression of SH2 has been observed in many cancers and isconsidered a prognostic marker. The phosphorylation process of SH2 activatesvariouscellularsignalingpathwayslikeRAS-MAPK,mTORandPI3K-AKT.Additionally, the role associating with RAS-MAPk pathway in proliferating tumorcells is well accepted. Protein tyrosine kinases and phosphatases are required toactivate these pathways and frequently over-activated in cancer cells. The SH2expressionwasshowntobenegativelyregulatedbySTAT3insometypesoftumorsa

ndalsotomediatetumorinvasionandmetastasisinthetumorcell.HencetargetingSH2 by developing potent inhibitors may reduce tumor cell growth and metastasis.(31).

2.REVIEWOFLITERATURE

A thorough literature survey was carried out on the investigation of the designand development of PARP1 and STAT3 dual inhibitors. The survey was limited totheperiodof2011 to 2020.

1. **Park *et al.,*** (2011) in this study, they examined the efficacy of NVP-BKM120, apan-class I PI3K inhibitor in human gastric cancer cells and hypothesized thatthecombinedinhibitionofPI3KandSTAT3wouldbesynergisticinKRASmutantgastric cancer cells. Compound 1 demonstrated anti-proliferative activity in 11humangastriccancercelllinesbydecreasingmTORdownstreamsignaling(32).

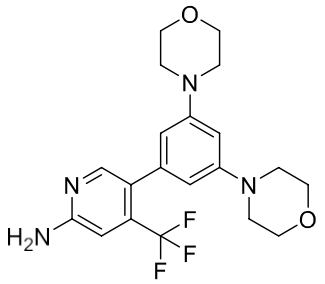

1

2. **Zeng *et al.,*** (2011) studied the Molecular modeling studies on benzimidazolecarboxamide derivatives as PARP-1 inhibitors Using 3D-QSAR and docking. Inthisstudy,moleculardockingand3D-QSARstudieswerecarriedoutnotonlytoexplore the interaction mechanism between 145 inhibitors and PARP-1 but alsoto construct highly accurate and predictive 3D-QSAR models, including theCoMFA (r2, 0.899; q2, 0.712 and CoMSIA (r2, 0.889; q2, 0.744, r2) modelsbased on flexible docking alignment, for predicting the biologic activity of newcompounds.Moleculardockingrevealsthe detailedstructures ofPARP-1bindingwith the compounds (33).
3. **Ye *et al.,*** (2013) described Design, Synthesis and Biological Evaluation of aSeriesofBenzo[de][1,7]naphthyridin-7(8H)-onesbearingafunctionalizedlonger chain appendage as novel PARP1 Inhibitors. A series of benzo[de][1,7]naphthyridin-7(8H)-one's derivatives have beendesignedandevaluatedasnovel PARP1 inhibitors. Initially, compound **2** bearing a terminal phthalazin-1(2H)-one framework and showing remarkably high PARP1 inhibitory

activity(0.31nM)butonlymoderatepotencyinthecell.Thefurthereffortgeneratedthe second-generationlead3showinghighpotencyagainstboththePARP1

enzymeandBRCA-deficientcells,especiallyfortheBRCA1-deficientMDA-MB-436cells (CC_{50}<0.26nM) (34).

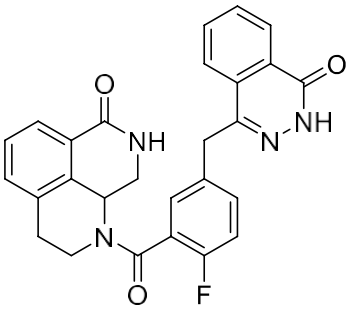

2

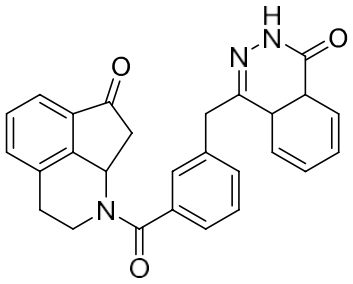

3

4. **Amin *et al.,*** (2013) described the synthesis, cytotoxic evaluation and moleculardocking study of novel quinazoline derivatives as PARP-1 inhibitors. There are16 compounds of spiro[(2H,3H)-quinazoline-2,1í-cyclohexane] derivatives thatwere designed and synthesized in this study. The synthesized compoundsevaluated for their *in-vitro* cellular evaluation against human breast carcinomacell lines (MCF-7) using doxorubicin as a reference drug. Most of the testedcompoundsdisplayedpromisingcytotoxicactivity,especiallyderivatives4,5and6are themost significantones(35).

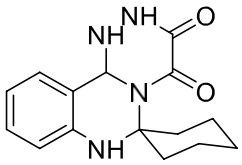

4

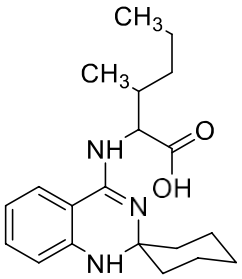

5

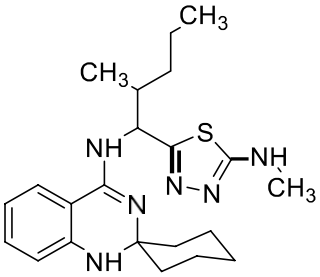

6

5. **Deepak*etal.,***(2013)designedaseriesoffluorinated3,6-diaryl-[1,2,4]triazolo[3,4-b][1,3,4]thiadiazolesandsynthesized.Thesynthesizedcompounds were screened for anticancer activity against three cancerous celllines MCF7 (human breast cancer), SaOS-2 (human osteosarcoma) and K562(humanmyeloidleukemia).Amongthese,compound**7**showedhigherantiproliferative activity (IC_{50}=22.1, 19 and 15 μM against MCF7, SaOS-2

andK562,respectively)while**7**exhibitedleastantiproliferativeactivity(IC_{50}=30.2,39 and29.4μMagainstMCF7,SaOS-2andK562cells,respectively)(36).

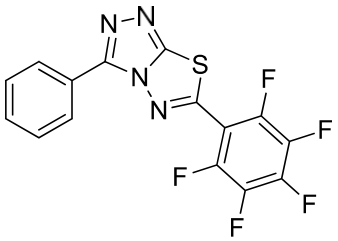

7

6. **Zhang *et al.,*** (2013) studied a new series of quinazoline derivatives weredesigned based on the reported synergistic effect between RTK and HDACinhibitors.Thesehybridsfeaturedthekeymoietiesofgefitiniborerlotinibaswell as the ZBG of HDACi. The inhibitory activities against HDAC, EGFR and HER2under cell-free conditions were evaluated. Almost all hybrids with hydroxamatesegments exhibited potent HDAC inhibitory activity. From the in-vitro studiescompound **8** showed similar anti-HDAC activities against HDAC1 (IC_{50}= 0.16μm),HDAC3(IC_{50}=0.18μm)andHDAC6(IC_{50}=0.56μm)(37).

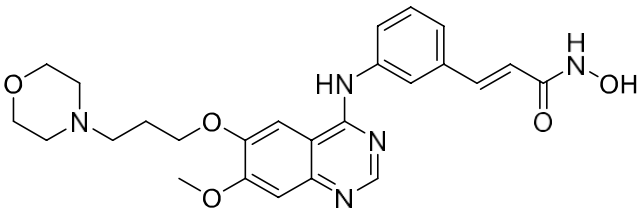

8

7. **Nan*etal.,***(2014)wasshownherethat2-[(aminocarbonyl)amino]-5-(4-fluorophenyl)-3-thiophenecarboxamide(**9**),apreviouslyreportedinhibitorofIkBkinases (IKK), blocked STAT3 recruitment to upstream kinases by docking intoSH2domainofSTAT3andattenuatedSTAT3activityinducedbycytokinesandcytoplasmictyrosinekinases.TPCA-1isaneffectiveinhibitorofSTAT3phosphorylation,DNAbinding,andtransactivation*invivo*.Itselectivelyrepressed the proliferation of NSCLC cells with constitutive STAT3 activation.Collectively,inthiswork,theauthorsidentified**9**asadirectdualinhibitorforbothIKKsandSTAT3(38).

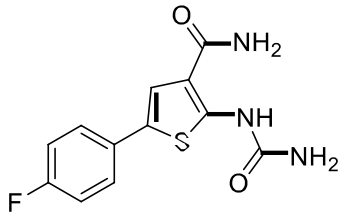

9

8. **Daka*etal.,***(2015)wasreportedthedesign,synthesisandevaluationofanovelclassof small-moleculeinhibitors,thatis,**10**anditsanalogs,aspromisingleadsfor further development of STAT3 inhibitors. Preliminary SARs was establishedfor **10** and its derivatives; and the binding modes were predicted by moleculardocking.LeadcompoundswithIC$_{50}$aslowas6.5μMinbreastcancercellline sand7.6μMinpancreaticcancercelllineswereidentified(39).

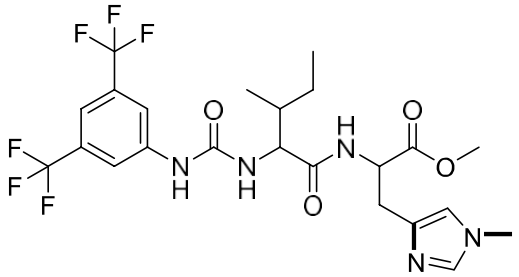

10

9. **Patel*etal.,***(2015)studiedtheDiscoveryandStructure−ActivityRelationshipofNovel 2,3Dihydrobenzofuran-7-carboxamideand2,3-Dihydrobenzofuran-3(2H)- one-7-carboxamide Derivatives as PARP- 1 Inhibitors. Novel substituted2,3-dihydro benzofuran-7-carboxamide (DHBF-7-carboxamide) and 2,3-dihydrobenzofuran-3(2H)-one-7-carboxamide(DHBF-3-one-7-carboxamide)derivatives were synthesized and evaluated as inhibitors of poly (ADP-ribose)polymerase-1 (PARP-1). A structure-based design strategy resulted in leadcompound**11**(DHBF-7-carboxamide;IC$_{50}$=9.45μM).Substituentslargerthanfluorine at the 5-position of the DHBF scaffold were found to be detrimental forPARP-1 inhibition. The 2-position methyl substitution is well tolerated in theDHBF-7-carboxamide scaffold **12** (IC$_{50}$ = 0.531 μM), yielding enantiomers thatbinddifferently in theactive site(40).

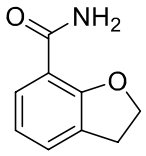

11

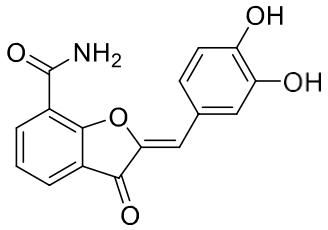

12

10. **Wang *et al.***, (2016) studied the design, synthesis, and biological evaluation ofnovelPARP-1InhibitorsBasedona1H-Thieno[3,4-d]Imidazole-4-CarboxamideScaffold.Inthisstudy,theauthorwasdesigned1H-thieno[3,4-d]imidazole-4-carboxamide moiety and synthesized it. These synthesized compounds wereundergone cellular evaluation and it indicated that the anti-cancer activities of13, 14, 15 and 16 against BRCA-deficient cell lines were similar to that ofolaparib, while the cytotoxicities of 3 and 4 toward human normal cells werelower(41).

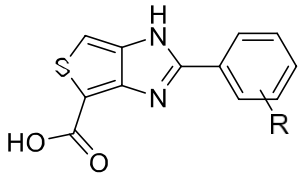

	R
13	**3-CF_3**
14	**4-NO_2**
15	**4-OCH_3**
16	**4-CH_3**

11. **Yang *et al.,*** (2016) Herein the authors describe a pharmacophore mergingstrategycombiningtheJAK2/FLT3inhibitorpacritnibwiththepan-HDACinhibitor, vorinostat, to create bispecific single molecules with both JAK andHDAC targeted inhibition. A preferred ether hydroxamate, 17 inhibits JAK2 andHDAC6 with low nanomolar potency, is <100nM potent against HDACs 2 and10, sub-micromolar potent against HDACs 1, 8 and 11, and >50 fold selectivefor JAK2 in a panel of 97 kinases. Broad cellular antiproliferative potency issupported by the demonstration of JAK-STAT and HDAC pathway blockade inseveral hematological cell lines, inhibition of colony formation in HEL cells, andanalysisof apoptosis (42).

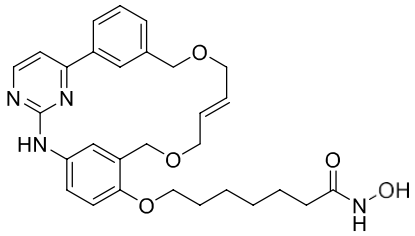

13

3.*AIMANDOBJECTIVES*

AIM

TodevelopadualinhibitorforPARP1andSTAT3enzymesandevaluation fortheiranti-cancerpotential.

OBJECTIVES

i. DesigningofdualinhibitorsbasedonDMLapproachesofknowninhibitorsofSTAT 3 andPARP1.

ii. In-silicoADMETpredictionandMoleculardockingstudies

iii. Thedesignedcompoundswillbesynthesizedinthelaboratorybytheconventional methods. Synthesized compounds will be characterized by IR,^{1}HNMR,LC-MS andelementalanalysis.

iv. *Invitro* anti-proliferativestudiesbyMTTassay.

4.PLANOF WORK

4.1. STAGEI:DESIGNING OFNOVELPARP1ANDSTAT3INHIBITORS

ThenicotinamidemovementofNAD$^+$isusedindevelopingPARP-1inhibitorstosimulatetheinteractionofNAD$^+$'ssubstratumprotein.Accordingtopriorresearch,the aromatic ring and carboxamide moiety are typical structural features of currentPARP1inhibitors,whicharenecessaryforhydrogenbondformationandpi-stackinginteraction with PARP-1. Veliparib is a highly effective PARP inhibitor used to treatseveral cancers with poor prognoses. Veliparib has been demonstrated to improvethe anti-tumor action of several damaging DNA agents, including temozolomide,cyclophosphamide,platinumandradiation,inpreclinicalmodelsofbreastandcoloncancer.InmanyclinicalstudiesofphasesIandII,Veliparibwasusedincombinationwithcarboplatintotreattriple-negativebreastcancer,andtheefficacyandsafetyofVeliparibinpatientswithbreastcancerweredemonstrated.Consideringthis,Veliparibisbeingtestedasananticanceragentagainstbreastcancerinthecurrentstudy.Asanewsmall-moleculeinhibitoroftheSTAT3signallingpathway,niclosamideis anFDA-approved anthelmintic drug. This compound effectivelyinhibited STAT3 activation and transcriptional function, Cells repair constitutivelyactivated STAT3 result in cell growth inhibition, death, and cell cycle arrest. Theamineringofbenzoylisthemostactivedrugareaofniclosamideandcanbeeasilyburdened to the enzyme and activity against breast cancer. Consequently, STAT3would be retained while possibly selective dual inhibitory action would develop byintroducingthebindinggroupforPARP1tothissite.Wethenaimedtotestinawiderange of solid tumors and hematological cell lines for PARP1-STAT3 inhibitors.Figure given below were depicts the schematic plans for the combined PARP1 andSTAT3 pharmacophore and development of new molecules as dual inhibitors forPARP1andSTAT3.**Figure9**showsthePlansformergedPARP1-STAT3pharmacophore.

4.2. **STAGEII:***DockingstudiesandADMETScreening*

- To carryout molecular docking studies for designed compounds by varioussoftware molecular modeling software's like Schrödinger, Discovery studio,PyRx and Auto-Dock software. Based on the results, we will select

thecompoundfor the synthesis.

- MMGBSAassaywillbecarriedoutforallthedesigned compounds.

- Molecularsimulation(dynamicstudy)willbecariedoutforthemos tactivecompounds.
- Theseleadswillfurtherbeevaluatedcomputationallyfortheir*ADMET*(A bsorption,Distribution,Metabolism,ExcretionandToxicity)profile.

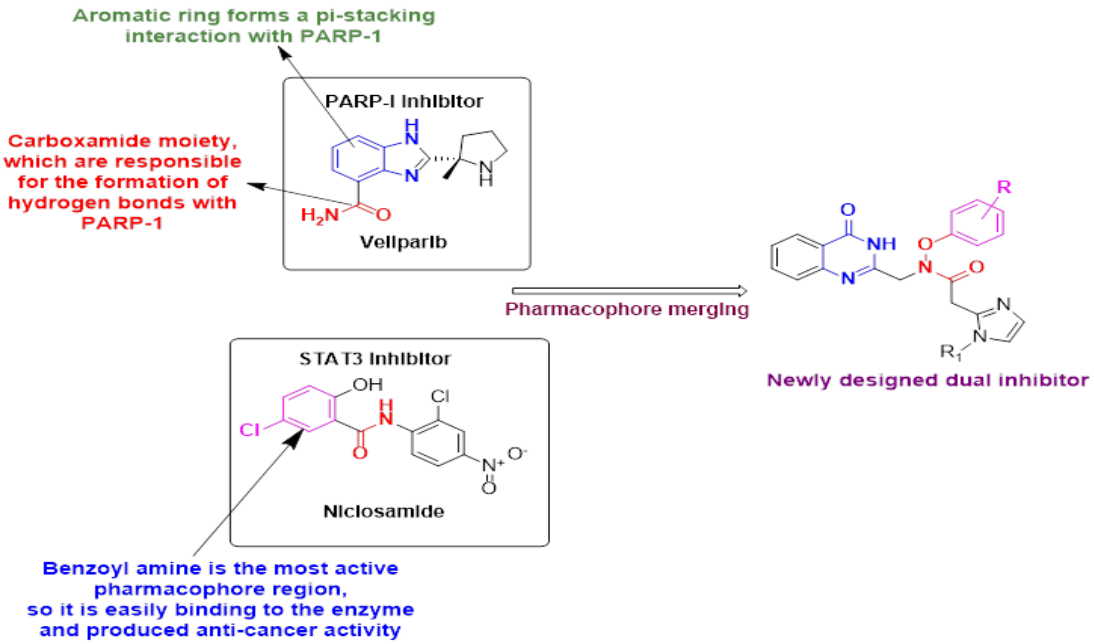

Figure9. PlansformergedPARP1-STAT3pharmacophore

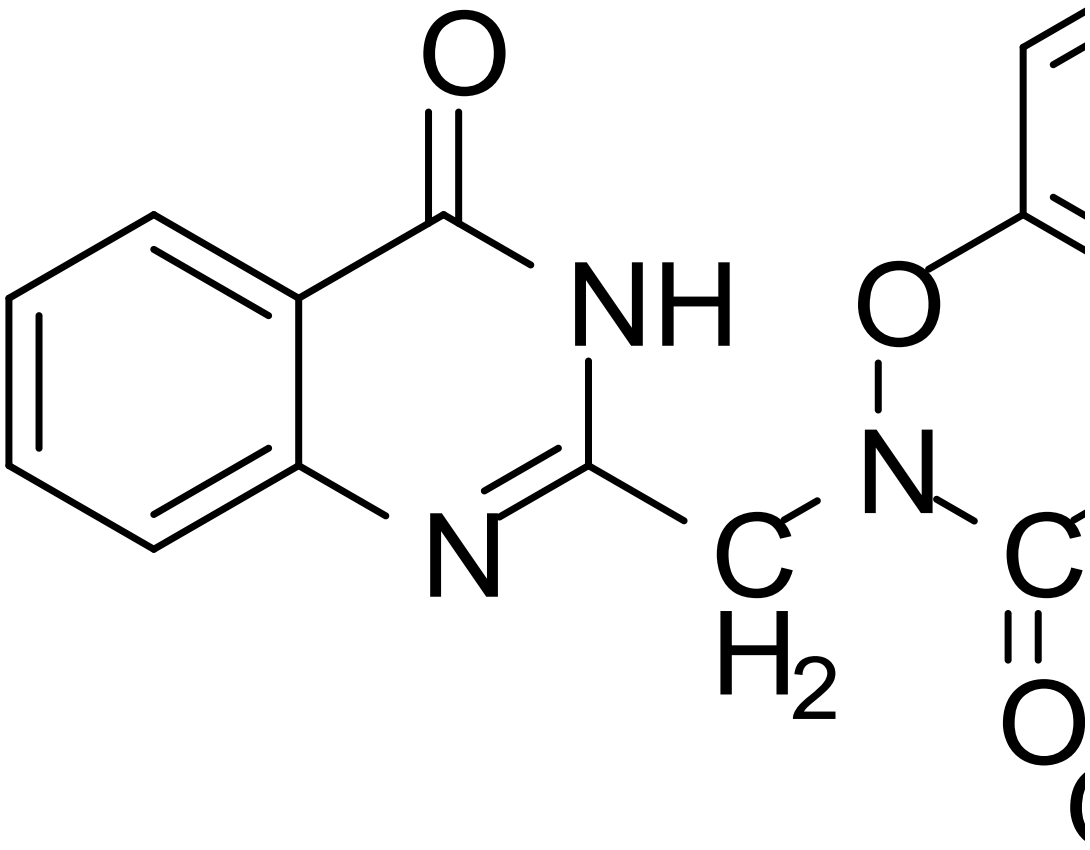

1d

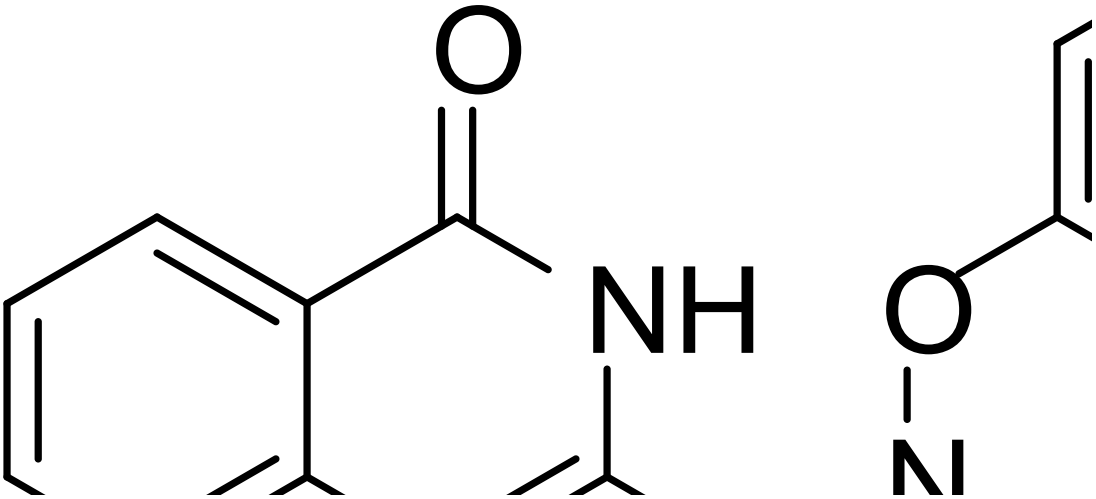

Figure 10. Newly designed Dual inhibitors

4.3. STAGEIII:*CHEMISTRY*

- Fromthesestudiestheleadmoleculeswillbeselectedforfurthersynthes is.
+
- Characterization of the synthesized compounds performed will be usingInfra-red (IR), Elemental analysis, Mass and Nuclear Magnetic Resonance(NMR) Spectroscopy.

4.4. STAGEIV:*INVITROCYTOTOXICEVALUATION*

- Antiproliferativeactivityofsynthesizedcompoundswillbeevaluatedby MTT assay usingselected celllines.

5. MATERIALS AND METHODS

5.1. Reagents and Instrumentation

- Oven dried glass wares were used to perform all the reactions. Procured reagents were of analytical grade and solvents of laboratory grade and purified as necessary according to techniques mentioned in Vogel's Textbook of Practical Organic Chemistry.
- In an open glass capillary tubes using Veego VMP-1 apparatus, melting points have been determined in ^{0}C and are uncorrected.
- Ascending TLC on precoated silica-gel plates (MERCK 6 F254) visualized under UV light was utilized to routinely monitor the progress and purity of the synthesized compounds. Solvents used during TLC are n-hexane, ethyl acetate, methanol, petroleum ether, chloroform and dichloromethane.
- The Infrared Spectra was plotted by Perkin-Elmer Fourier Transform-Infrared
  Spectrometer and in reciprocal centimeters the band positions are noted.
- Nuclear magnetic spectra (^{1}H NMR) were obtained from Bruker DRX-300 (300 MHz FT-NMR) spectrophotometer using DMSO as solvent with TMS as the internal standard^{13}C NMR have been recorded utilizing Bruker with Dimethyl sulphoxide as solvent. Shimadzu LC-MS was employed to record Mass Spectra.

5.2. Molecular Docking

Geometrically optimized with Chem Sketch 12.01 software are used for drawing of 2-(1-substituted-1H-benzo[d]imidazol-2-yl]-N acetamide derivatives. LigPrep was responsible for optimizing the prepared ligands (Schrodinger Suite 2018-2). Every energy-minimized analog was employed in LigPrep as the input structure. PARP1 (PDB ID: 4ZZZ, resolution 1.90) and STAT3 (PDB ID: 6NJS, resolution 2.70) were both prepared using Maestro's Protein Preparation Wizard, Schrodinger Suite 2018-2. All water molecules that do not interact with the ligand and are more than 5Å distant from the ligand have been eliminated from the crystallographic molecules of water. The atoms missing in the side loop of the protein structure were added using Prime (Schrodinger 2018-2). Hydrogen bonds

have been provided for all amino acid residues at pH 7.0 taking into account the minimum ionization states. To ease the steric obstruction the energy reduction was achieved by applying the OPLS-3 force field to achieve the Root Mean Square Deviation of 0.30 livres. As the active location, the co-crystal coordinates which already exist in the protein were employed and a center grid box was used to build the binding pocket. The pocket-size produced is proportional to the co-crystal size. Compounds have been inserted into the resultant grid box following optimization with Glide (Schrodinger suite 2018-2), eliminating all constraints. Compounds have been optimized with LigPrep. Then Glide values were analyzed to choose compounds. Then Glide Scores were analyzed and compounds were selected for further studies.

5.3. In silico ADMET Prediction

A pharmacokinetic property (ADMET) of created C1-C15 compounds using Qikprop was predicted in a computational trial (Schrodinger 2018-2). We calculated the molecular volumes (MV) and molecular weights for hydrogen bond (MW), the number of acceptors of hydrogen bond (N-OHNH), the total activity of the CNS, the percent of oral human absorption, the polar surface area (PSA), the constant distribution of 1-octyl alcohol-water (log P o/w), the permeability of the cell of the Caco-2 cells and MDCK. The stated characteristics help understand all drug/synthesized molecules' ADME characteristics. Also known were pharmacological similarities, five-specific and three-specific infringements. A molecule to be used by mouth should be distributed with a consistent distribution of 5 molecular mass per 500, the number of donors of H-bonds per 5 and the number of receiving ones of H-bonds per 10 and only one breach of the conditions mentioned above is permissible.

5.4. In vitro anti-cancer evaluation

5.4.1. Cell culture and conditions

The ATCC cell lines A-549, MCF-7, and MDA-MB-231 were maintained in DMEM with 10% FBS, 100 U/mL penicillin, and 100 g/mL streptomycin. The cells were cultured at 37°C and 5% CO_2.

5.4.2. MTT assay

MTT (3-(4,5 dimethyl thiazole-2yl)-2,5-diphenyl tetrazolium bromide) tetrazolium salt should be cleaved, according to the principle. The amount of

formazan produced by the cells utilized was found to be related to the number of cells used. Using DMEM media containing 10% FBS, the cell culture was adjusted to 1.0105 cells/mL. 100L distilled cell suspension (about 10,000 cells/well) was put to each well of a 96 well flat bottom microtitre plate. After the cell population was determined to be sufficient after 24 hours, the cells were centrifuged, and the pellets were suspended in maintenance media containing 100L of various test sample concentrations. The plates were incubated for 48 hours at 37 degrees Celsius in a 5 percent CO_2, with observations collected every 24 hours. MTT (2mg/mL) in MEM-PR (MEM without phenol red) was added after 48 hours. At 37°C for 2 hours, the plates were incubated (5 percent CO_2 atmosphere). The plates were agitated to solubilize the produced formazan after adding 100 L of DMSO. A microplate reader was used to measure the absorbance at a wavelength of 540 nm. The formula was used to calculate the percentage of cells that were viable.

$$\%\text{Cell viability} = \frac{\text{Mean OD of individual sample}}{\text{Mean OD of control}} \times 100$$

5.5. Chemistry

5.5.1.Synthesis of 2-chloro-N-((4-oxo-3,4-dihydroquinazolin-2-yl)methyl)acetamide (A)

In a 50 mL round bottom flask, substituted aniline/amino thiazole (6 mmol) was dissolved in THF (5 ml). To this solution, DBU (1.2 mmol) was added. The reaction mixture was placed on freezing mixture of ice and salt & mechanically stirred for 15 min. To this reaction mixture, chloroacetyl chloride (6.1 m mol) was added from dropping funnel at such rate that the temperature does not rise beyond 5oC. After allchloroacetyl chloride was added to the reaction mixture, it was stirred for 3-6 h at rt. The progress of reaction was monitored by TLC (Hexane: EtOAc; 7:3). After completion, the reaction mixture was poured into cold water. The compound was precipitated out. This was filtered and washed with water. The precipitate was dried and recrystallized by using ethanol as solvent. The product was obtained as solid powder.

5.5.2. Step 2: Synthesis of N-((4-oxo-3,4-dihydroquinazolin-2-yl)methyl)-2-phenoxy acetamide

The various substituted phenol derivatives (094gm, 10mmole) were taken in a flask containing 10mL of dichloromethane. To this add compound A (1.18gm, 15mmole) in dichloromethane was added dropwise and the reaction mixture was stirred at room temperature for 4hr. After 4hr of stirring the reaction mixture was taken into ether, washed with 20& NaOH solution, 10% HCl and saturated sodium bicarbonate solution and it was dried over anhydrous sodium sulfate. The solvent was evaporated to get final product N-((4-oxo-3,4-dihydroquinazolin-2-yl)methyl)-2-phenoxyacetamide (B1-B10).

5.5.3. Step 3: Preparation of imidazole-2-yl acetic acid

Hydrazine (0.1mmol) diamine condensed in 25 mL of 4N HCl with malonic acid (0.05mmol). Reflux was used with stirring for 4 hours at 850C. TLC observed the reaction in a mobile phase with Ethyl acetate: n-Hexane (7:3). Ammonia was added to the reaction mixture after completing the reaction (monitored by TLC). The resulting substance was filtered and dried. After recrystallization of the crude product with ethanol, the corresponding product was

produced in high purity.

5.5.4. Step 4: synthesis of 2-(1-substituted-1H-imidazol-2-yl)acetic acid (C1 – C3)

A mixture of 2(1-H-benzimidazol-2-yl) acetic acid (0.01mol) in 40 ml DMF was added to the mixture of substituted acid chloride (0.012 mol) in triethylamine (0.012mol). Reaction mixtures were refluxed for 1h at 150-155^{0}C until the starting material disappeared by TLC. After the reaction was completed, the precipitate formed upon cooling and it was filtered and recrystallized from ethanol to achieve the final compounds (C1-C3).

5.5.5. Step 5: Synthesis of Final compounds

The equimolar concentration of B1-B10 (1mmol) and C1 – C3 were mixed with $SOCl_2$ (1mmol) and stirred at room temperature for 5–20 minutes using triethylamine (3mmol) in dichloromethane as a catalyst. The reaction solvent was evaporated after the TLC check and the residue received was washed with 1 N HCl and 1 NaOH. The organic phase (Na_2SO_4) was dried and dried to ensure that the relevant carboxylic amide derivatives were available (C1-15).

5.6. In vitro anti-cancer evaluation

5.6.1. Cell culture and conditions

The ATCC cell lines A-549, MCF-7, and MDA-MB-231 were maintained in DMEM with 10% FBS, 100 U/mL penicillin, and 100 g/mL streptomycin. The cells were cultured at 37°C and 5% CO_2.

5.6.2. MTT assay

MTT (3-(4,5 dimethyl thiazole-2yl)-2,5-diphenyl tetrazolium bromide) tetrazolium salt should be cleaved, according to the principle. The amount of formazan produced by the cells utilized was found to be related to the number of cells used. Using DMEM media containing 10% FBS, the cell culture was adjusted to 1.0105 cells/mL. 100L distilled cell suspension (about 10,000 cells/well) was put to each well of a 96 well flat bottom microtitre plate. After the cell population was determined to be sufficient after 24 hours, the cells were centrifuged, and the pellets were suspended in maintenance media containing 100L of various test sample concentrations. The plates were incubated for 48 hours at 37 degrees Celsius in a 5 percent CO_2, with observations collected every 24 hours. MTT (2mg/mL) in MEM-PR (MEM without phenol red) was added after 48 hours. At 37°C for 2 hours, the plates were incubated (5 percent CO_2 atmosphere). The plates were agitated to solubilize the produced formazan after adding 100 L of DMSO. A microplate reader was used to measure the absorbance at a wavelength of 540 nm. The formula was used to calculate the percentage of cells that were viable.

$$\%\text{Cell viability} = \frac{\text{Mean OD of individual sample}}{\text{Mean OD of control}} \times 100$$

6. RESULT AND DISCUSSION

6.1. Molecular Docking

The in-silico docking study of the designed molecules to the enzyme's active sites was performed by the Glide module of Schrodinger suit-2018-2 for determining the binding affinities of the ligands. The designed compounds were docked towards the PARP1 and STAT3 in order to ascertain their PARP1 and STAT3 inhibition activity against breast cancer. All the compounds exhibited good affinity to the receptor when compared with standard drugs like veliparib and niclosamide with PARP1 and STAT3 inhibitory activity as an anti-breast cancer agent. The Glide energy of docking studies against PARP1 (PDB ID: 4ZZZ) and STAT3 (PDB ID: 6JNS) are shown in table 1 and table 2 respectively. From the in-silico docking results, it is evident that the interactions are mainly lipophilic factors due to the presence of aromatic heterocyclic rings. The roles of certain crucial amino acids in the ligand-binding domain of the PARP1 and STAT3 inhibitors were also established. Major non-covalent interactions between the studied ligands and the ligand-binding domain of the PARP1 and STAT3 inhibitors were investigated. These amino acids have been repeatedly implicated during ligand interaction with the PARP1 and STAT3 inhibitors and also play important role in the inhibition of the ligand-binding domain of PARP1 and STAT3 inhibitors.

Table1.The Glide energy of docking studies against PARP1

Title	glide gscore	glide evdw	glide ecoul	glide energy	glide emodel	XP HBond
1d	**-9.914**	**-66.159**	**-15.691**	**-81.851**	**-133.672**	**-1.890**
1e	-10.811	-58.733	-13.989	-72.722	-128.824	-1.890
1f	**-8.689**	**-67.770**	**-17.824**	**-85.594**	**-145.062**	**-2.028**
1g	-10.004	-65.801	-11.333	-77.135	-131.315	-1.614
1h	-11.180	-54.561	-16.779	-71.341	-114.381	-2.053
1i	-7.919	-58.956	-7.248	-66.204	-105.237	-1.178
1j	-9.801	-61.951	-12.682	-74.634	-108.692	-1.575
1k	-12.123	-58.751	-17.705	-76.456	-127.308	-2.909
1l	-11.349	-64.792	-13.615	-78.408	-122.897	-1.784

1m	**-10.788**	**-64.248**	**-15.195**	**-79.444**	**-136.260**	**-1.890**
2d	-9.165	-61.883	-14.352	-76.235	-129.615	-1.890
2e	-11.067	-61.364	-15.818	-77.182	-127.927	-1.816
2f	-10.957	-61.837	-16.213	-78.049	-129.550	-1.737
2g	-9.313	-58.605	-16.459	-75.064	-127.509	-1.851
2h	-11.349	-64.792	-13.615	-78.408	-122.897	-1.784
2i	-8.925	-58.001	-18.776	-76.777	-124.542	-1.811
2j	-6.611	-57.944	-4.951	-62.895	-100.501	-0.577
2k	**-8.293**	**-64.346**	**-16.146**	**-80.492**	**-133.758**	**-1.720**
2l	**-11.933**	**-67.089**	**-15.432**	**-82.521**	**-136.309**	**-2.315**
2m	**-10.788**	**-64.248**	**-15.195**	**-79.444**	**-136.260**	**-1.890**
3d	-11.194	-58.773	-13.775	-72.548	-113.179	-1.890
3e	-11.596	-61.496	-15.931	-77.427	-119.332	-2.486
3f	-10.203	-62.492	-13.893	-76.385	-130.908	-1.793
3g	**-11.044**	**-67.879**	**-14.485**	**-82.364**	**-141.013**	**-1.696**
3h	**-9.865**	**-65.145**	**-16.877**	**-82.022**	**-145.260**	**-1.890**
3i	-10.636	-59.319	-13.357	-72.676	-116.485	-1.488
3j	**-10.154**	**-64.029**	**-15.827**	**-79.856**	**-134.296**	**-1.890**
3k	**-6.018**	**-62.792**	**-17.579**	**-80.371**	**-119.726**	**-1.890**
3l	-12.123	-58.751	-17.705	-76.456	-127.308	-2.909
3m	-11.349	-64.792	-13.615	-78.408	-122.897	-1.784

Among the docked compounds, compound 1f possesses highest glide energy **-85.594** k/cal compared to standard drug veliparib -57.76 k/cal. The compound 1f shows 3 hydrogen bonds between the ketone group of ligands with amino acid Gly863 and Ser904, Hydrogen of amine with amino acid Gly863 and it also showing pi-pi interaction between Tyr 907 with quinazoline moiety which is similar to standard drug veliparib. The compound 2l, 3g, and 3h shows good glide energy -82.521 k/cal, -82.364 k/cal and -82.022 k/cal respectively. The compound 2l showing 4 hydrogen bonds between the ketone group of ligands with amino acid Gly863 and Ser904, Hydrogen of amine with amino acid Gly863 Nitrogen atom from nitro group with amino acid Arg 865 and it also showing pi-pi interaction between Tyr 907 with quinazoline moiety. Remaining docked compounds showing glide energy range from -36 to -50 K/cal along with one or

two hydrogen bond interaction and Pi-Pi interaction. The **figure 11 – 20**shows that 2D docking pose of ligands 1d, 1f, 1m, 2k, 2l, 2m, 3g, 3h, 3j, and 3k respectively.

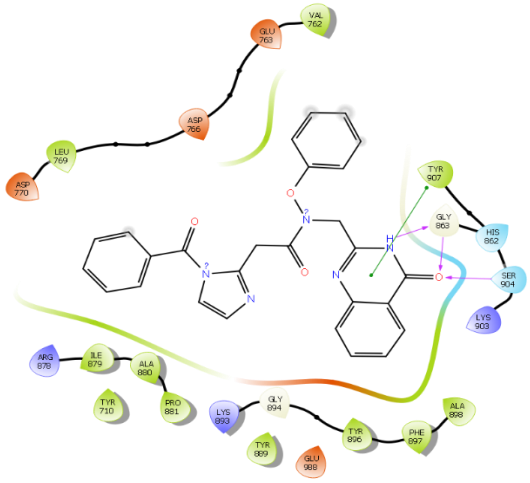

Figure 11. Fitting pose interactions of compound 1d in the pocket of **4ZZZ** in 2D view.

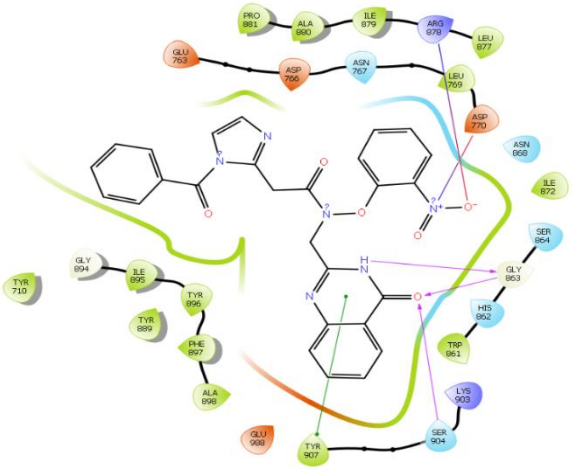

Figure 12. Fitting pose interactions of compound 1f in the pocket of **4ZZZ** in 2D view.

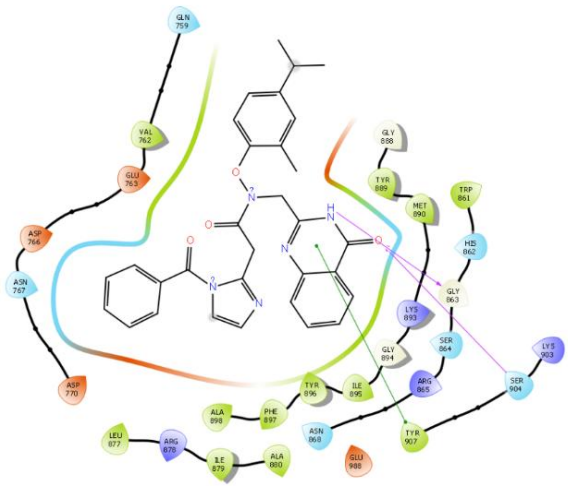

Figure 13. Fitting pose interactions of compound 1m in the pocket of **4ZZZ** in 2D view.

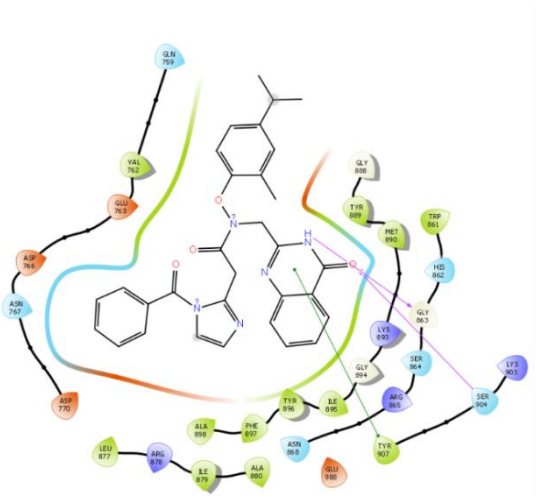

Figure 14. Fitting pose interactions of compound 2k in the pocket of **4ZZZ** in 2D view.

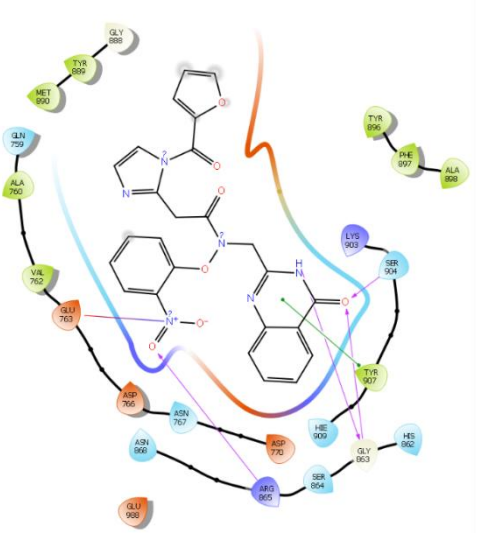

Figure 15. Fitting pose interactions of compound 2l in the pocket of **4ZZZ** in 2D view.

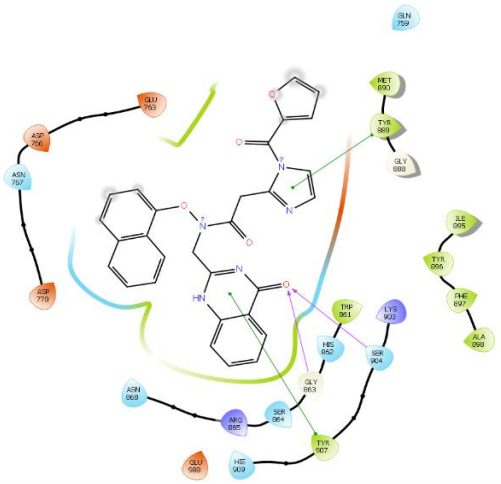

Figure 16. Fitting pose interactions of compound 2m in the pocket of **4ZZZ** in 2Dview.

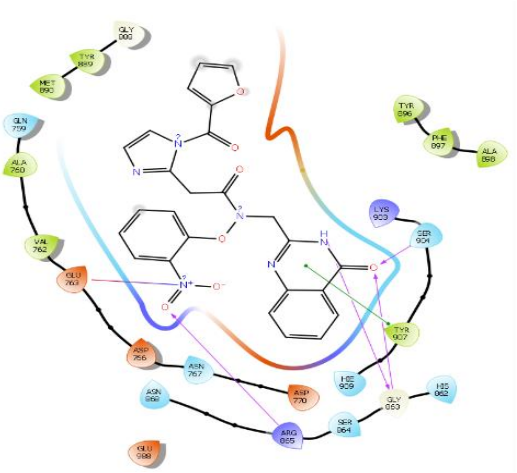

Figure 17. Fitting pose interactions of compound 3g in the pocket of **4ZZZ** in 2D view.

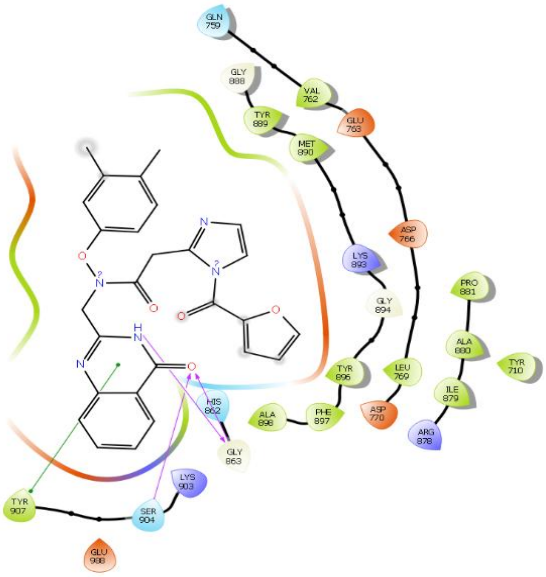

Figure 18. Fitting pose interactions of compound 3h in the pocket of **4ZZZ** in 2D view.

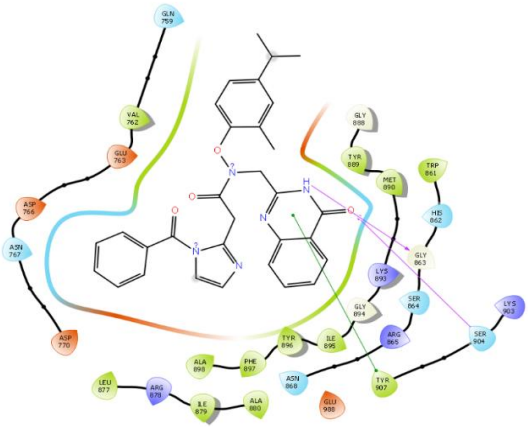

Figure 19. Fitting pose interactions of compound 3j in the pocket of **4ZZZ** in 2D

view.

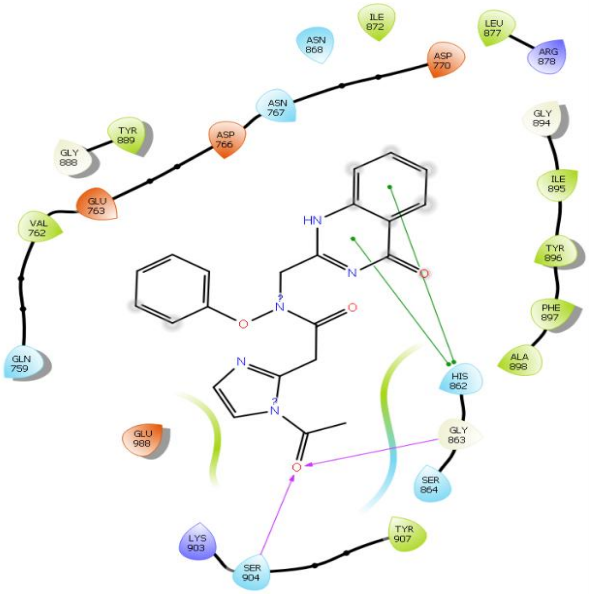

Figure 20. Fitting pose interactions of compound 3k in the pocket of **4ZZZ** in 2D view.

Results of docking studies of STAT3 enzyme shows the compound 1f shows similar glide energy -85.59 k/cal compared to standard drug niclosamide -51.27 K/cal. The compound 1f produced two conventional hydrogen bonds between Try640 with oxygen atom of nitro group and oxygen atom of keto group. The derivatives 2l, 3g, and 3h shows a significant glide energy -82.521 k/cal, -82.364, and -82.022 k/cal respectively along with two conventional hydrogen bonds between amino acids Try640 and Try657 with oxygen atom of keto group respectively and it also makes two Pi-Pi interaction between Try640 with quinazoline ring and furan moiety. Remaining docked compounds showing glide energy range from -62 to -81 K/cal along with one or two hydrogen bond interaction and Pi-Pi interaction. The **figure 21 – 30**shows that 2D docking pose of ligands 1d, 1f, 1m, 2k, 2l, 2m, 3g, 3h, 3j, and 3k respectively.

Table 2. The Glide energy of docking studies against STAT3

Title	glide G score	glide evdw	glide ecoul	glide energy	glide einternal	glide emodel	XP HBond
1d	**-9.914**	**-66.159**	**-15.691**	**-81.851**	**7.906**	**-133.672**	**-1.890**
1e	-10.811	-58.733	-13.989	-72.722	2.575	-128.824	-1.890
1f	**-8.689**	**-67.770**	**-17.824**	**-85.594**	**4.436**	**-145.062**	**-2.028**
1g	-10.004	-65.801	-11.333	-77.135	10.899	-131.315	-1.614

1h	-11.180	-54.561	-16.779	-71.341	13.676	-114.381	-2.053
1i	-7.919	-58.956	-7.248	-66.204	15.398	-105.237	-1.178
1j	-9.801	-61.951	-12.682	-74.634	11.747	-108.692	-1.575
1k	-12.123	-58.751	-17.705	-76.456	13.905	-127.308	-2.909
1l	-11.349	-64.792	-13.615	-78.408	8.641	-122.897	-1.784
1m	**-10.788**	**-64.248**	**-15.195**	**-79.444**	**6.017**	**-136.260**	**-1.890**
2d	-9.165	-61.883	-14.352	-76.235	9.292	-129.615	-1.890
2e	-11.067	-61.364	-15.818	-77.182	10.655	-127.927	-1.816
2f	-10.957	-61.837	-16.213	-78.049	4.393	-129.550	-1.737
2g	-9.313	-58.605	-16.459	-75.064	4.936	-127.509	-1.851
2h	-11.349	-64.792	-13.615	-78.408	8.641	-122.897	-1.784
2i	-8.925	-58.001	-18.776	-76.777	3.216	-124.542	-1.811
2j	-6.611	-57.944	-4.951	-62.895	2.282	-100.501	-0.577
2k	**-8.293**	**-64.346**	**-16.146**	**-80.492**	**13.648**	**-133.758**	**-1.720**
2l	**-11.933**	**-67.089**	**-15.432**	**-82.521**	**17.823**	**-136.309**	**-2.315**
2m	**-10.788**	**-64.248**	**-15.195**	**-79.444**	**6.017**	**-136.260**	**-1.890**
3d	-11.194	-58.773	-13.775	-72.548	9.091	-113.179	-1.890
3e	-11.596	-61.496	-15.931	-77.427	16.876	-119.332	-2.486
3f	-10.203	-62.492	-13.893	-76.385	0.000	-130.908	-1.793
3g	**-11.044**	**-67.879**	**-14.485**	**-82.364**	**9.243**	**-141.013**	**-1.696**
3h	**-9.865**	**-65.145**	**-16.877**	**-82.022**	**3.229**	**-145.260**	**-1.890**
3i	-10.636	-59.319	-13.357	-72.676	7.087	-116.485	-1.488
3j	**-10.154**	**-64.029**	**-15.827**	**-79.856**	**8.856**	**-134.296**	**-1.890**
3k	**-6.018**	**-62.792**	**-17.579**	**-80.371**	**4.010**	**-119.726**	**-1.890**
3l	-12.123	-58.751	-17.705	-76.456	13.905	-127.308	-2.909
3m	-11.349	-64.792	-13.615	-78.408	8.641	-122.897	-1.784

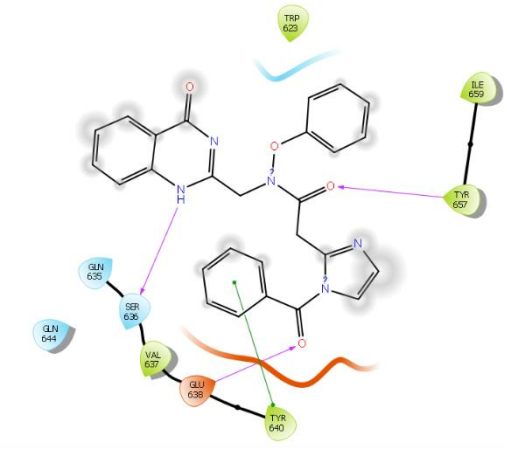

Figure 21. Fitting pose interactions of compound 1d in the pocket of **6NJS** in 2D view.

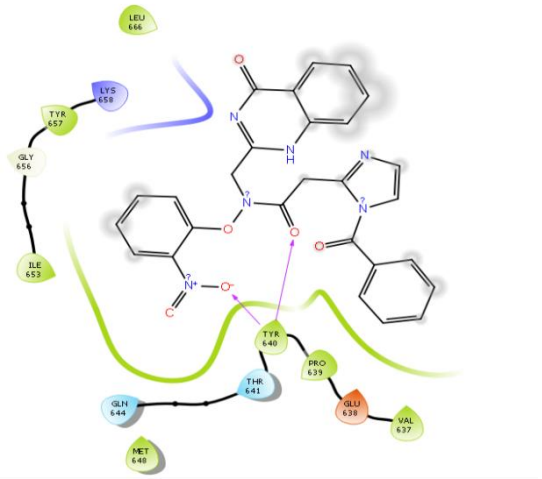

Figure 22. Fitting pose interactions of compound 1f in the pocket of **6NJS** in 2D view.

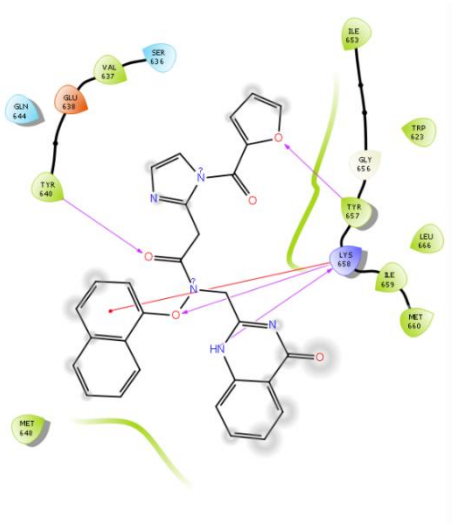

Figure 23. Fitting pose interactions of compound 1m in the pocket of **6NJS** in 2D view.

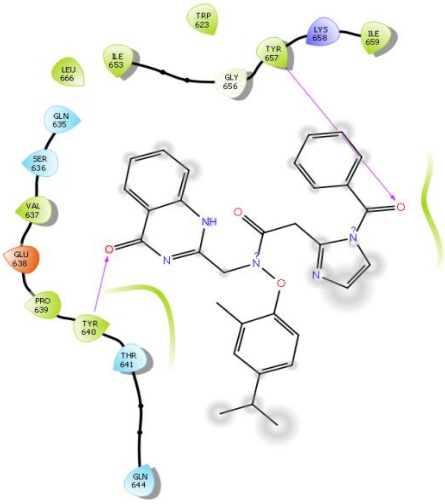

Figure 24. Fitting pose interactions of compound 2k in the pocket of **6NJS** in 2D view.

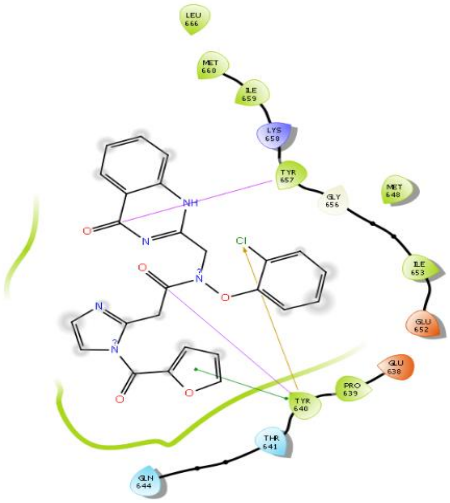

Figure 25. Fitting pose interactions of compound 2l in the pocket of **6NJS** in 2D view.

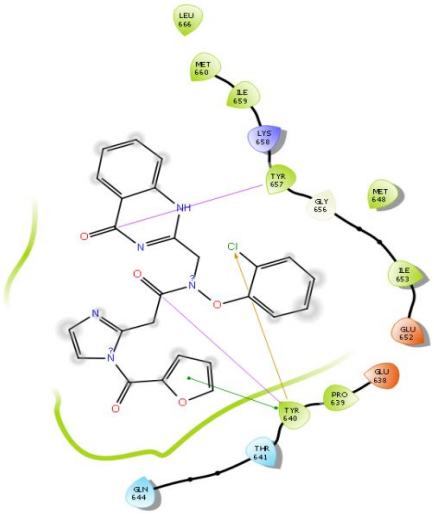

Figure 26. Fitting pose interactions of compound 2m in the pocket of **6NJS** in 2D view.

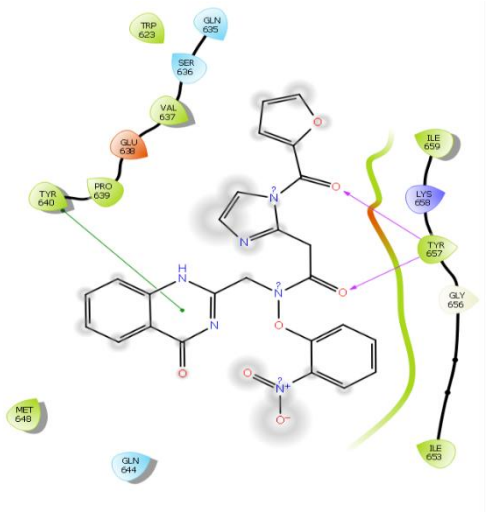

Figure 27. Fitting pose interactions of compound 3g in the pocket of **6NJS** in 2D view.

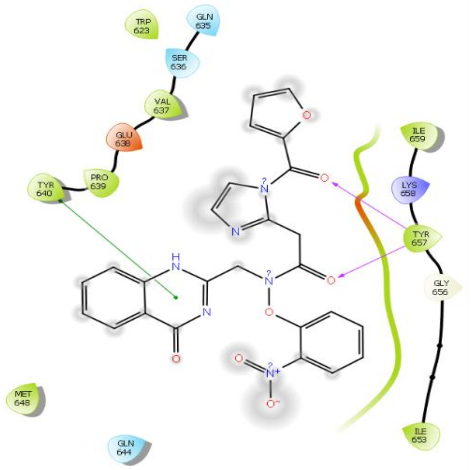

Figure 28. Fitting pose interactions of compound 3h in the pocket of **6NJS** in 2D view.

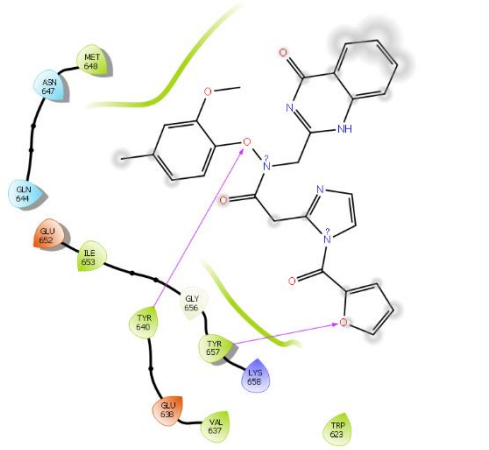

Figure 29. Fitting pose interactions of compound 3j in the pocket of **6NJS** in 2D view.

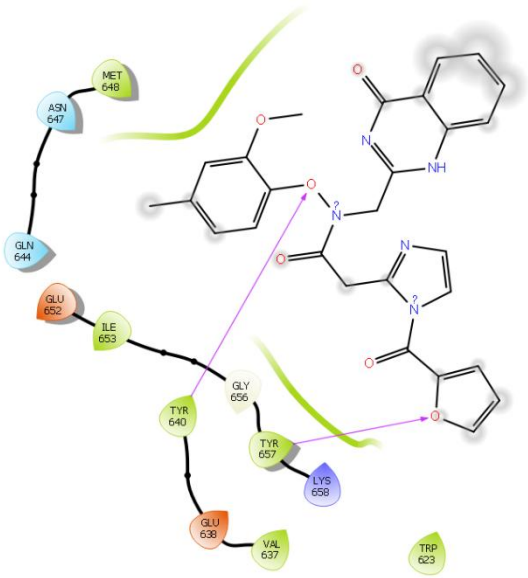

Figure 30. Fitting pose interactions of compound 3k in the pocket of **6NJS** in 2D view.

6.2. In-silico ADMET Prediction.

The in-silico ADMET properties of the designed ligands was determined by Qikprop module of Schrödinger suite 2018-2. Molecular weight of the designed compounds ranged between 475 to 535. The estimated no. of hydrogen bonds donors was in the range of 1-2. The estimated no. of hydrogen bonds acceptors was between 7- 9.7. The predicted octanol/water partition coefficient were in the range of 11 to 12 and the number of likely metabolic reactions between 3-5. There are one parameter violations of Lipinski's rule of five was found in all molecule. All the compounds have 65 to 95 % Human Oral Absorption. So almost all the properties of the compounds are within the recommended values. The details of the *in-silico* ADMET properties for the quinazolinone based derivatives were shown in the **Table 3**.

Table 3. The details of the *in-silico* ADMET properties for the quinazolinone based derivatives

Title	MW	Donor HB	Acpt HB	Log P o/w	metab	% Human oral absorption	Rule of Five
1d	479.49	1	11	2.689	3	83.987	0
1e	513.93	1	11	2.813	3	76.706	1

1f	524.49	1	12	1.900	4	84.996	2
1g	493.52	1	11	3.050	4	96.355	0
1h	431.450	1	11	1.902	4	87.074	0
1i	523.54	1	11	2.672	5	78.751	1
1j	461.47	1	11	2.045	5	84.874	0
1k	433.42	2	11	0.815	4	66.535	0
1l	467.48	1	11	2.518	3	88.358	0
1m	519.51	1	11	3.128	4	76.688	1
2d	469.45	1	11	2.353	4	91.978	0
2e	499.48	1	12	2.207	5	77.298	1
2f	462.42	1	12	0.842	4	83.667	1
2g	483.48	1	11	2.457	5	86.277	0
2h	467.48	1	11	2.518	3	88.358	0
2i	445.47	1	11	1.617	5	83.150	0
2j	473.53	1	11	2.607	5	87.581	0
2k	535.60	1	11	4.189	5	90.287	1
2l	485.45	2	12	1.587	5	60.700	1
2m	519.51	1	11	3.128	4	76.688	1
3d	417.42	1	11	1.498	3	82.949	0
3e	447.44	1	11	1.756	4	83.277	0
3f	503.90	1	11	1.944	4	70.653	1
3g	514.45	1	12	1.442	5	80.390	2
3h	497.50	1	11	2.263	6	88.192	0
3i	445.47	1	11	1.617	5	83.150	0
3j	513.50	1	12	2.504	6	66.092	2
3k	525.56	1	11	2.686	6	74.197	1

6.3. Synthetic work

Based on SAR studies of previously available PARP-1 and STAT3 inhibitors such as veliparib and niclosamide, the compounds was designed for synthesis. As per scheme all the compounds were synthesized conventionally. All the compounds and intermediates were purified by successive recrystallization from ethanol. The IR spectrum of the final synthesized compounds showed absorption bands around 3566.93 – 3340.74 cm^{-1} for amide

NH, while the distinguishing broad absorption peaks C=O for CONH were observed in the range 1635.69 cm^{-1}, 3566.93- 3340.74 cm^{-1} for NH, 3467.16 cm^{-1} for OH acid, 1350.69–1464 cm^{-1} for CN, 1379– 1344 cm^{-1} for CH3, and 800–700 cm^{-1} for aromatic ring. These compounds also exhibited appropriate peaks at corresponding δ ppm in their ^{1}H NMR spectra. The ^{1}H NMR spectra of the synthesized compounds revealed singlet signal at 10.39 for H of OH, doublet signal at 3.38 – 3.35 for H of CH_2, signal at 6.9-8.5 for H of aromatic ring. The figure 17- 88 shows the IR, 1H NMR, and mass spectra for all synthesized compounds. All the synthesized compounds were subjected for docking studies, in-vitro cytotoxicity study using breast cancer cell lines.

6.3.1. - 2-(1-benzoyl-1H-imidazol-2-yl)-N-((4-oxo-3,4-dihydroquinazolin-2-yl)methyl)-N-phenoxyacetamide (1d)

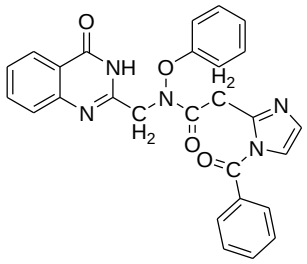

$C_{27}H_{21}N_5O_4$; Exact Mass: 479.16: Molecular Weight: 479.50: m/z: 479.16 (100.0%), 480.16 (29.2%), 481.17 (4.1%), 480.16 (1.8%): Elemental Analysis: C, 67.63; H, 4.41; N, 14.61; O, 13.35: ^{1}H NMR (500 MHz, DMSO) δ 8.09 (s, 3H), 7.69 – 7.57 (m, 6H), 7.57 – 7.43 (m, 12H), 7.43 – 7.37 (m, 9H), 7.23 (s, 3H), 7.14 – 7.09 (m, 6H), 6.88 (t, *J* = 1.5 Hz, 1H), 6.87 – 6.74 (m, 8H), 6.28 (s, 3H), 5.15 (s, 3H), 4.21 (s, 3H), 4.11 – 4.07 (m, 6H).

6.3.2. 2-(1-benzoyl-1H-imidazol-2-yl)-N-(2-chlorophenoxy)-N-((4-oxo-3,4-dihydroquinazolin-2-yl)methyl)acetamide (1f)

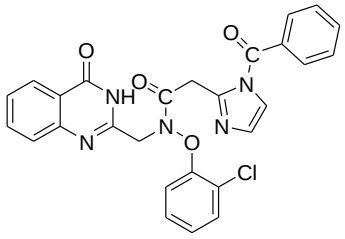

$C_{27}H_{20}ClN_5O_4$: Exact Mass: 513.12: Molecular Weight: 513.94: m/z: 513.12 (100.0%), 515.12 (32.0%), 514.12 (29.2%), 516.12 (9.3%), 515.13 (4.1%), 514.12 (1.8%), 517.12 (1.3%): Elemental Analysis: C, 63.10; H, 3.92; Cl, 6.90; N, 13.63; O, 12.45: **ir**3200 (NH stretching 2^{0} amine), 1651 (C=O stretching amine), 1450 (C-N bending), 927 (Aromatic ring) ^{1}H NMR (500 MHz, DMSO) δ 8.06 (s,

1H), 7.80 – 7.68 (m, 2H), 7.60 (s, 1H), 7.49 (t, J = 12.4 Hz, 3H), 7.44 – 7.38 (m, 2H), 7.35 (s, 1H), 7.23 (s, 1H), 7.10 (s, 1H), 6.97 (s, 1H), 6.75 (s, 1H), 6.69 (s, 1H), 4.90 (s, 1H), 4.28 (s, 1H), 4.06 – 4.02 (m, 2H).

6.3.3. 2-(1-benzoyl-1H-imidazol-2-yl)-N-(naphthalen-2-yloxy)-N-((4-oxo-3,4-dihydroquinazolin-2-yl)methyl)acetamide

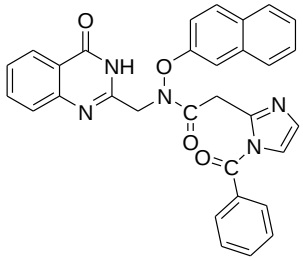

Chemical Formula: $C_{31}H_{23}N_5O_4$: Exact Mass: 529.18: Molecular Weight: 529.56: m/z: 529.18 (100.0%), 530.18 (33.5%), 531.18 (2.7%), 531.18 (2.7%), 530.17 (1.8%): Elemental Analysis: C, 70.31; H, 4.38; N, 13.23; O, 12.08: **ir** 3279 (NH stretching 2^0 amine), 1637 (C=O stretching amide), 1407 (C-N bending), 923 (Aromatic ring) ^{1}H NMR (500 MHz, DMSO) δ 7.89 (d, J = 30.6 Hz, 6H), 7.72 (d, J = 0.5 Hz, 6H), 7.67 – 7.57 (m, 6H), 7.57 – 7.54 (m, 5H), 7.44 (t, J = 11.0 Hz, 10H), 7.39 – 7.26 (m, 18H), 7.23 (s, 3H), 7.07 (s, 3H), 4.75 (s, 3H), 4.53 (s, 3H), 3.98 – 3.94 (m, 6H).

6.3.4. 2-(1-(furan-2-carbonyl)-1H-imidazol-2-yl)-N-(3-isopropyl-2-methylphenoxy)-N-((4-oxo-3,4-dihydroquinazolin-2-yl)methyl)acetamide (2k)

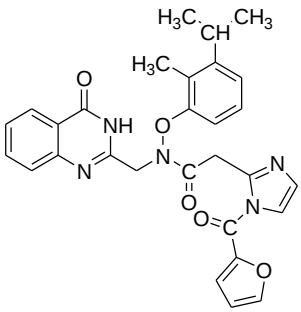

$C_{29}H_{27}N_5O_5$: Exact Mass: 525.20: Molecular Weight: 525.57: m/z: 525.20 (100.0%), 526.20 (31.4%), 527.21 (2.7%), 527.21 (2.0%), 526.20 (1.8%), 527.21 (1.0%): Elemental Analysis: C, 66.28; H, 5.18; N, 13.33; O, 15.22: **ir 2917** (C=O stretching aromatic), 1680 (C=O stretching amide), 1419 (C-N bending), 932 (Aromatic ring) ^{1}H NMR (500 MHz, Chloroform) δ 8.04 (s, 1H), 7.65 (s, 1H), 7.51 (t, J = 8.6 Hz, 3H), 7.38 (s, 1H), 7.16 (s, 1H), 7.02 (d, J = 18.4 Hz, 2H), 6.84 (d, J = 28.4 Hz, 2H), 6.50 (s, 1H), 5.66 (s, 1H), 4.93 (s, 1H), 3.96 (s, 1H), 3.79 (m, 2H), 3.03 (s, 1H), 2.22 (m, 3H), 1.29 (m, 6H).

6.3.5. 2-(1-(furan-2-carbonyl)-1H-imidazol-2-yl)-N-(3-hydroxyphenoxy)-N-((4-oxo-3,4-dihydroquinazolin-2-yl)methyl)acetamide (2l)

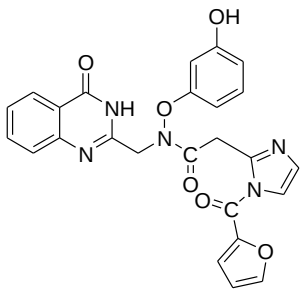

$C_{25}H_{19}N_5O_6$: Exact Mass: 485.13: Molecular Weight: 485.46: m/z: 485.13 (100.0%), 486.14 (27.0%), 487.14 (2.7%), 486.13 (1.8%), 487.14 (1.2%): Elemental Analysis: C, 61.85; H, 3.95; N, 14.43; O, 19.77: **ir**3348 (NH stretching 2^oamine), 3227 (C=H stretching aromatic) 1668 (C=O stretching amide) 1403 (C-N bending) 905 (aromatic ring) ^{1}H NMR (500 MHz, DMSO) δ 9.42 (s, 1H), 8.06 (s, 1H), 7.57 (d, J = 32.3 Hz, 2H), 7.51 (s, 1H), 7.44 (s, 1H), 7.30 (s, 1H), 7.12 (s, 1H), 7.07 (s, 1H), 6.98 (s, 1H), 6.46 (dd, J = 25.5, 9.2 Hz, 4H), 6.17 (s, 1H), 4.63 (s, 1H), 4.03 – 3.99 (m, 2H), 3.85 (s, 1H), -0.55 (s, 1H).

6.3.6. 2-(1-(furan-2-carbonyl)-1H-imidazol-2-yl)-N-(naphthalen-2-yloxy)-N-((4-oxo-3,4-dihydroquinazolin-2-yl)methyl)acetamide (2m)

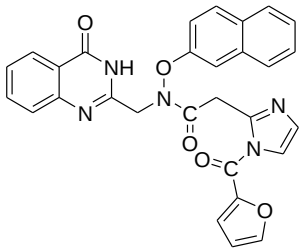

$C_{29}H_{21}N_5O_5$: Exact Mass: 519.15: Molecular Weight: 519.52: m/z: 519.15 (100.0%), 520.16 (31.4%), 521.16 (2.7%), 521.16 (2.0%), 520.15 (1.8%), 521.16 (1.0%): Elemental Analysis: C, 67.05; H, 4.07; N, 13.48; O, 15.40: **ir**3388 (NH stretching 2^0amine) 3160 (C-H stretching aromatic) 1697 (C=O stretching amide) 1453 (C-N bending) 875 (Aromatic ring)^{1}H NMR (500 MHz, DMSO) δ 7.90 (d, J = 27.6 Hz, 6H), 7.77 – 7.62 (m, 9H), 7.49 (dd, J = 45.4, 7.6 Hz, 10H), 7.42 (s, 5H), 7.34 – 7.24 (m, 9H), 7.22 (s, 3H), 7.05 (s, 3H), 6.52 (s, 3H), 5.92 (s, 3H), 4.83 (s, 3H), 4.61 (s, 3H), 4.15 (m, 6H).

6.3.7. 2-(1-acetyl-1H-imidazol-2-yl)-N-(2-nitrophenoxy)-N-((4-oxo-3,4-

dihydroquinazolin-2-yl)methyl)acetamide (3g)

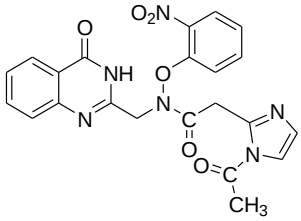

$C_{22}H_{18}N_6O_6$: Exact Mass: 462.13: Molecular Weight: 462.42: m/z: 462.13 (100.0%), 463.13 (23.8%), 464.14 (2.7%), 463.13 (2.2%), 464.13 (1.2%): Elemental Analysis: C, 57.14; H, 3.92; N, 18.17; O, 20.76: **ir 3409** (NH stretching 2^0 amine) 3165 (C=H stretching aromatic) 1659 (C=O stretching amide) 1406 (C-N bending) 921 (Aromatic) ^{1}H NMR (500 MHz, DMSO) δ 8.05 (d, J = 30.9 Hz, 4H), 7.98 (s, 2H), 7.52 – 7.38 (m, 8H), 7.36 (s, 2H), 7.15 (d, J = 20.5 Hz, 5H), 7.13 – 7.05 (m, 2H), 7.04 (s, 3H), 5.22 (s, 2H), 4.10 (m, 4H), 4.00 (s, 2H), 2.12 (m, 6H).

6.3.8. 2-(1-acetyl-1H-imidazol-2-yl)-N-((4-oxo-3,4-dihydroquinazolin-2-yl)methyl)-N-(o-tolyloxy)acetamide (3h)

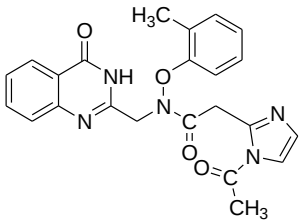

$C_{23}H_{21}N_5O_4$: Exact Mass: 431.16: Molecular Weight: 431.45: m/z: 431.16 (100.0%), 432.16 (24.9%), 433.17 (3.0%), 432.16 (1.8%): Elemental Analysis: C, 64.03; H, 4.91; N, 16.23; O, 14.83: **ir** 2962 (C=O stretching aromatic) 1417 (C-N bending) ^{1}H NMR (500 MHz, DMSO) δ 8.14 (s, 1H), 8.03 (s, 1H), 7.54 (s, 1H), 7.48 (d, J = 13.6 Hz, 2H), 7.35 (s, 1H), 7.16 (s, 1H), 7.00 (d, J = 17.7 Hz, 2H), 6.94 (s, 1H), 6.78 (s, 1H), 4.81 (s, 1H), 4.19 (s, 1H), 3.97 (m, 2H), 2.37 (m, 6H).

6.3.9. 2-(1-acetyl-1H-imidazol-2-yl)-N-(2-methoxy-3-methylphenoxy)-N-((4-oxo-3,4-dihydroquinazolin-2-yl)methyl)acetamide (3j)

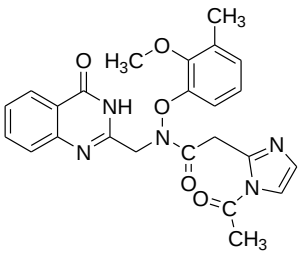

$C_{24}H_{23}N_5O_5$: Exact Mass: 461.17: Molecular Weight: 461.48: m/z: 461.17 (100.0%), 462.17 (26.0%), 463.18 (2.7%), 462.17 (1.8%), 463.17 (1.0%): Elemental Analysis: C, 62.47; H, 5.02; N, 15.18; O, 17.33: **ir** 3400 (NH stretching 2^0 amine) 1652 (C=O stretching amide) 994 (Aromatic ring) ^{1}H NMR (500 MHz, DMSO) δ

8.54 (s, 1H), 8.05 (s, 1H), 7.65 – 7.47 (m, 3H), 7.36 (s, 1H), 7.17 (s, 1H), 6.79 (s, 1H), 6.69 (d, J = 18.8 Hz, 2H), 4.84 (s, 1H), 4.42 (s, 1H), 4.05 – 4.01 (m, 2H), 3.88 – 3.84 (m, 3H), 2.37 – 2.29 (m, 6H).

6.3.10. 2-(1-acetyl-1H-imidazol-2-yl)-N-(3-isopropyl-2-methylphenoxy)-N-((4-oxo-3,4-dihydroquinazolin-2-yl)methyl)acetamide (3k)

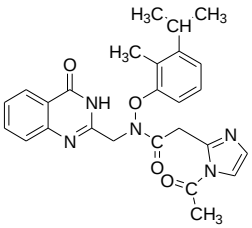

$C_{26}H_{27}N_5O_4$: Exact Mass: 473.21: Molecular Weight: 473.53: m/z: 473.21 (100.0%), 474.21 (28.1%), 475.21 (2.7%), 474.20 (1.8%), 475.21 (1.1%): Elemental Analysis: C, 65.95; H, 5.75; N, 14.79; O, 13.51: **ir**^{1}H NMR (500 MHz, DMSO) δ 8.05 (s, 1H), 7.55 (d, J = 0.9 Hz, 2H), 7.49 (s, 1H), 7.36 (s, 1H), 7.17 (s, 1H), 7.04 (s, 1H), 6.86 (s, 1H), 6.63 (s, 1H), 5.67 (s, 1H), 5.06 (s, 1H), 4.17 (m, 2H), 4.06 (s, 1H), 3.07 (s, 1H), 2.42 (m, 3H), 2.33 (m, 3H), 1.38 (m, 6H).

6.4.Spectral Data For synthesized compounds

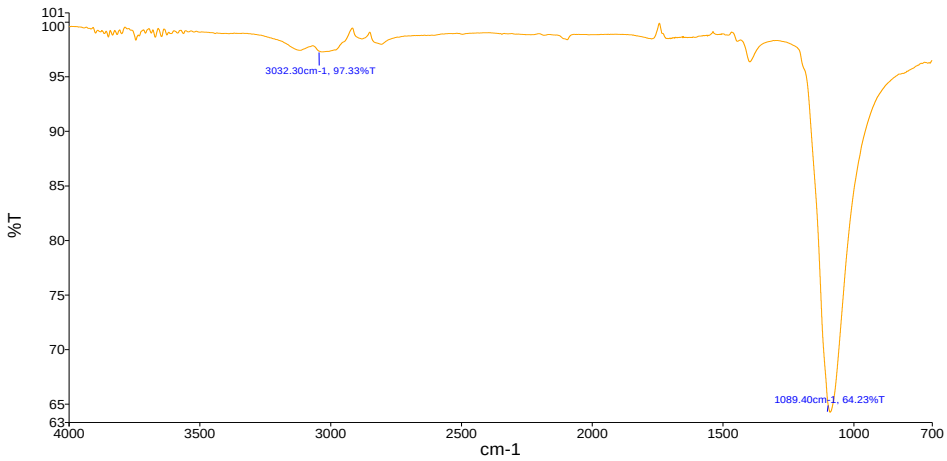

Figure 31: IR spectra for compound 1d

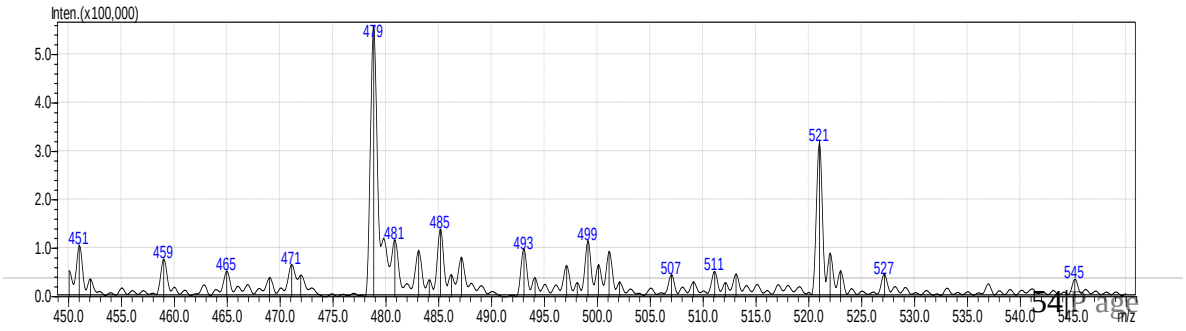

Figure 32: Mass spectra for compound 1d

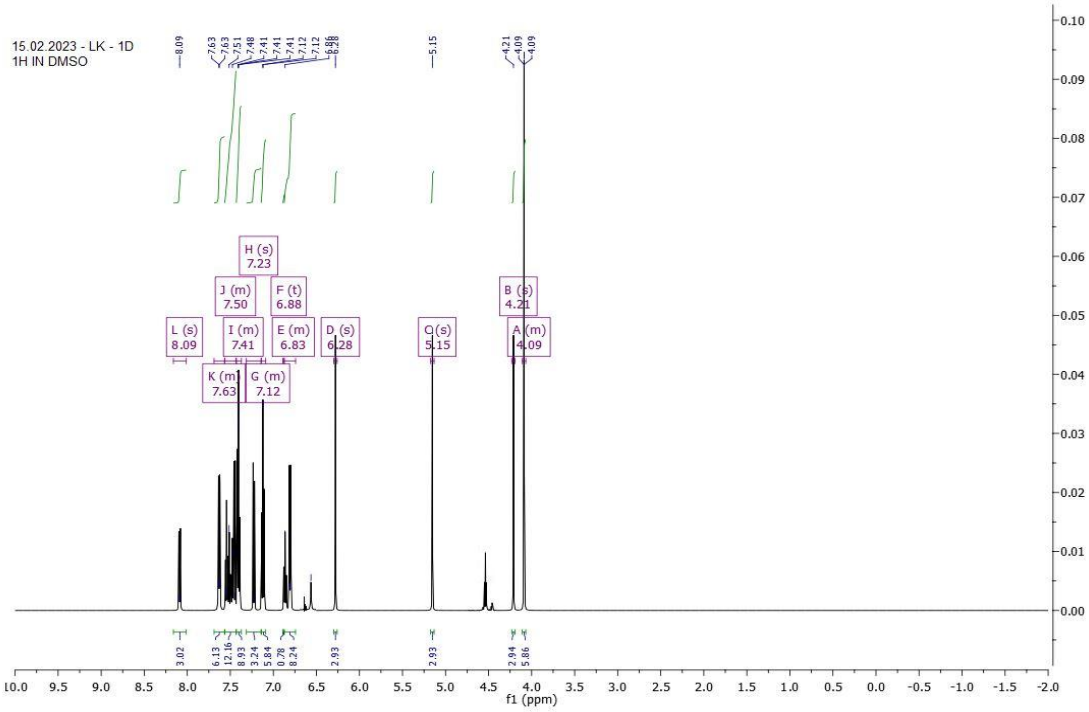

Figure 33: ^{1}H NMR for compound 1d

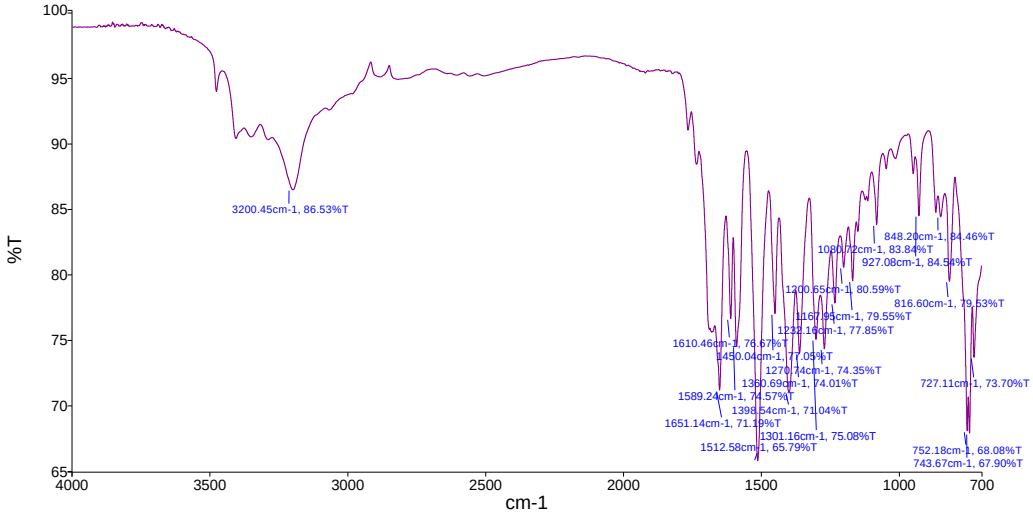

Figure 34: IR spectra for compound 1f

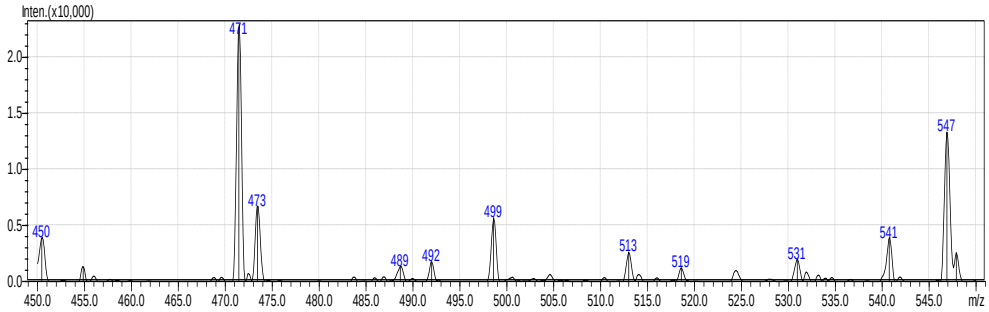

Figure 35: Mass spectra for compound 1f

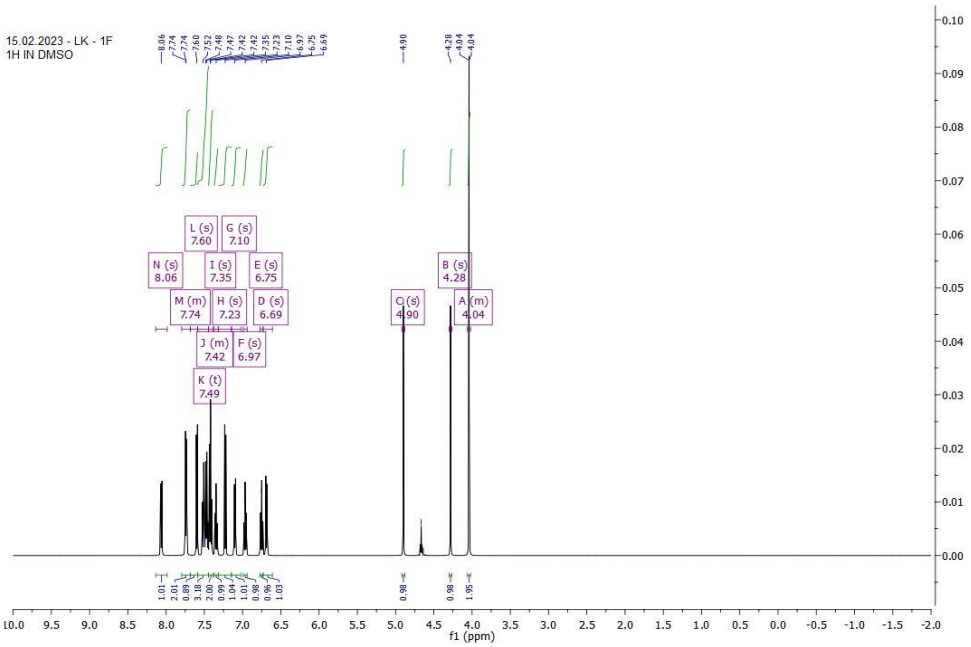

Figure 36: ^{1}H NMR for compound 1f

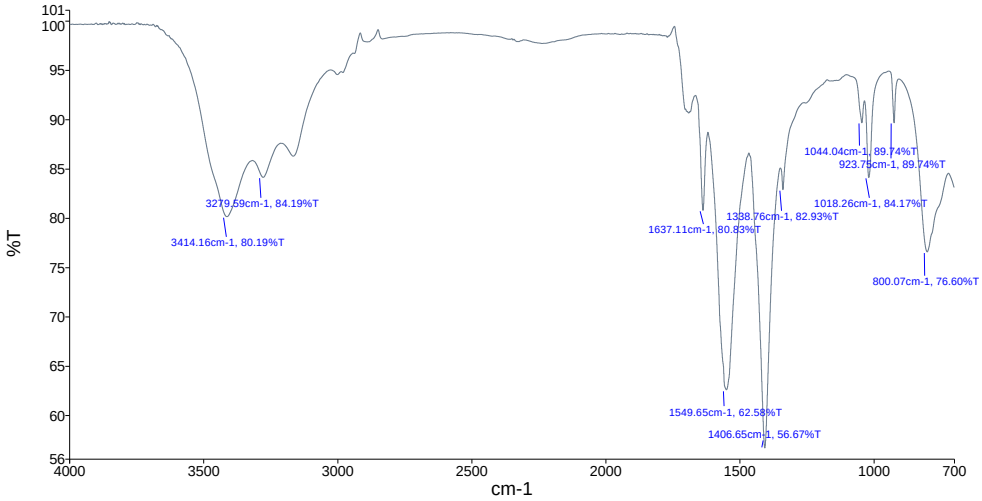

Figure 37: IR spectra for compound 1m

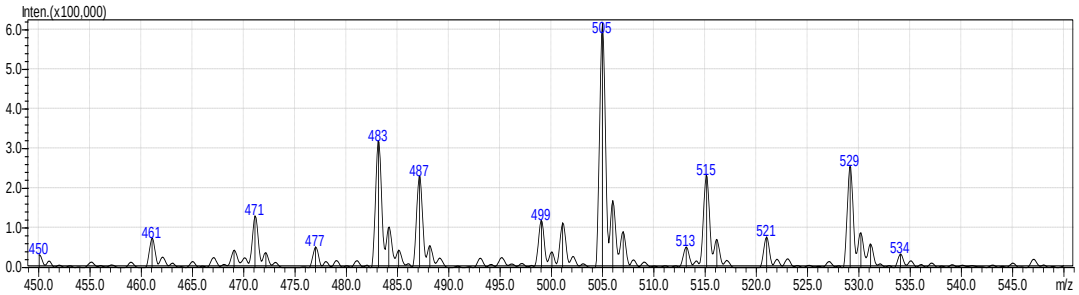

Figure 38: Mass spectra for compound 1m

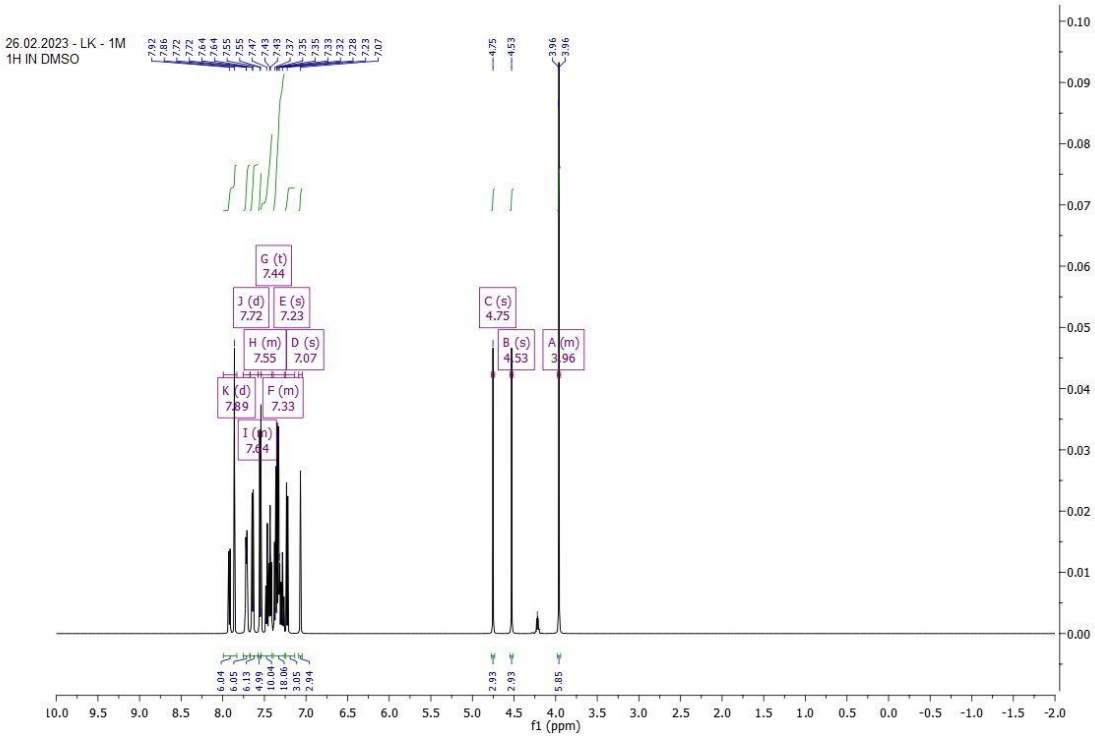

Figure 39: ^{1}H NMR for compound 1m

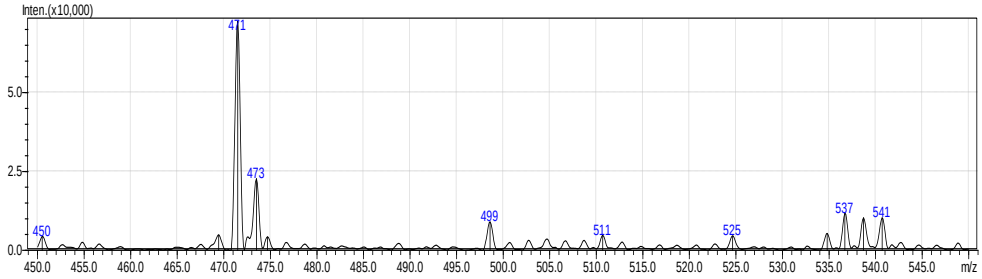

Figure 40: IR spectra for compound 2k

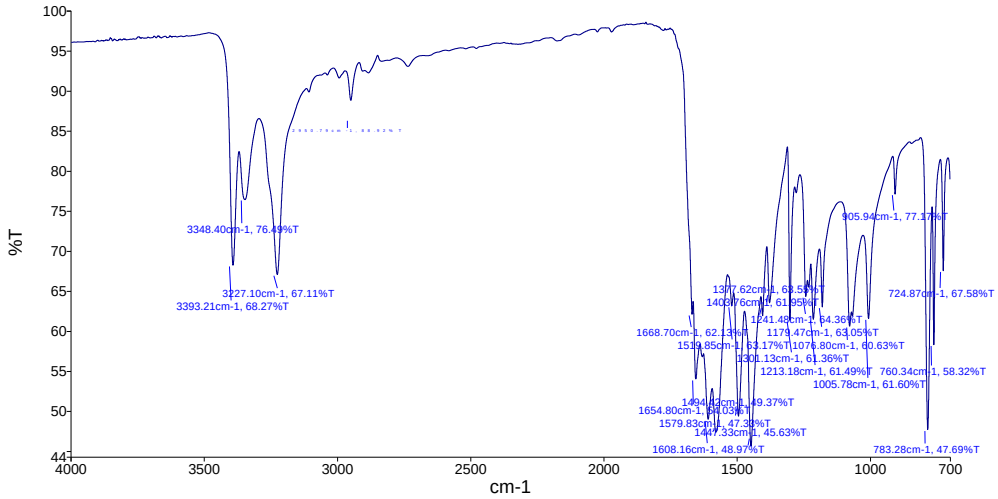

Figure 41: Mass spectra for compound 2k

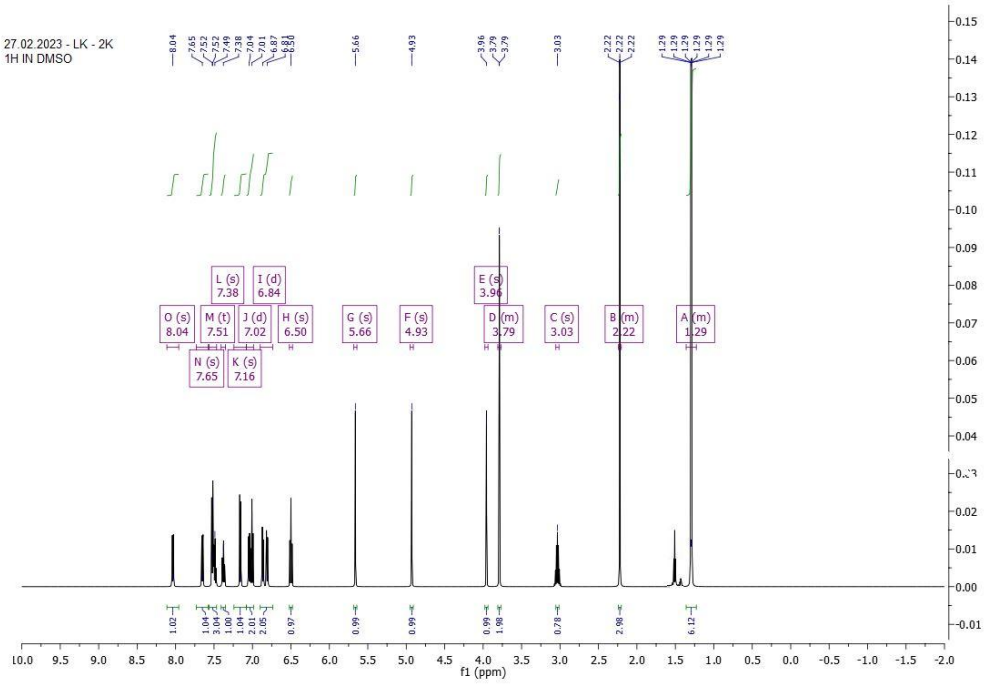

Figure 42: ^{1}H NMR for compound 2k

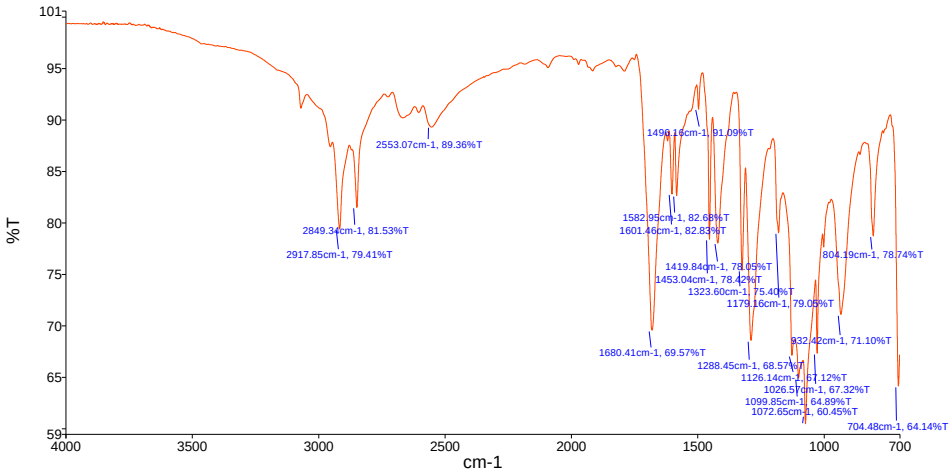

Figure 43: IR spectra for compound 2l

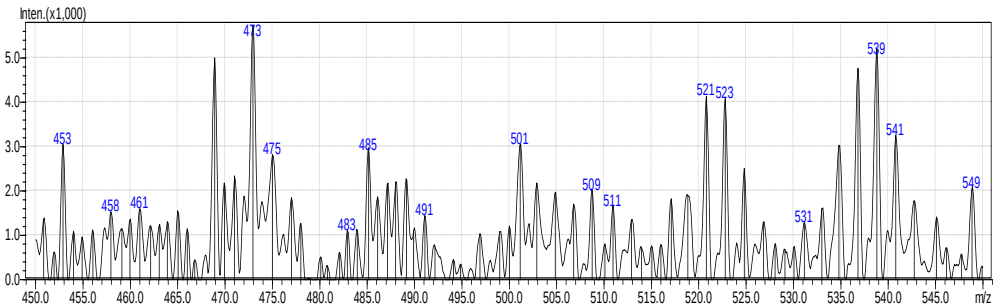

Figure 44: Mass spectra for compound 2l

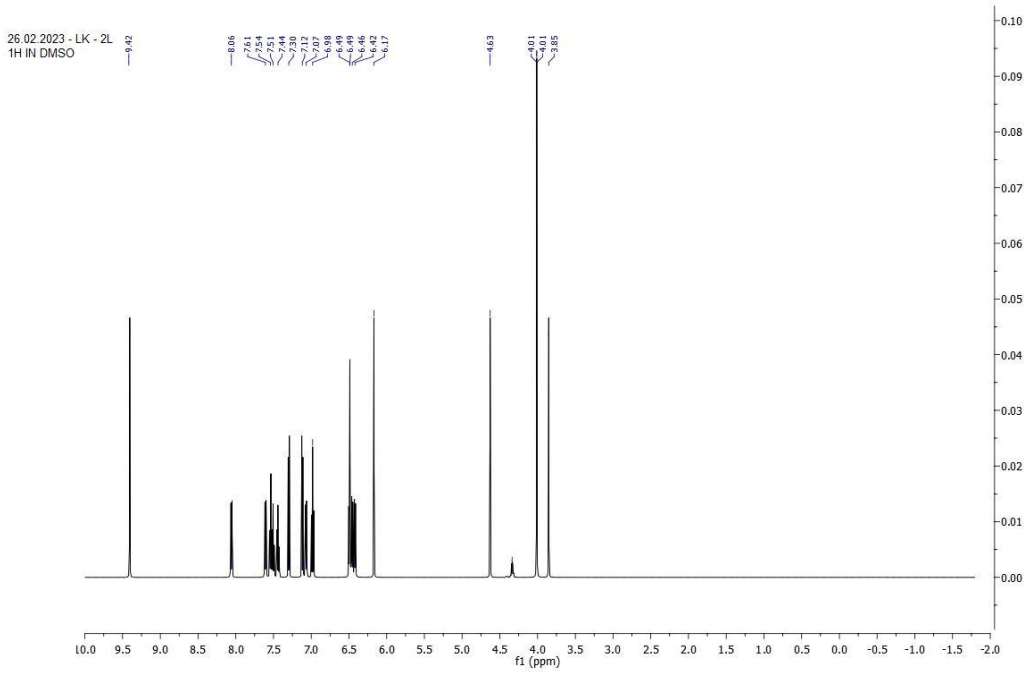

Figure 45: ^{1}H NMR for compound 2l

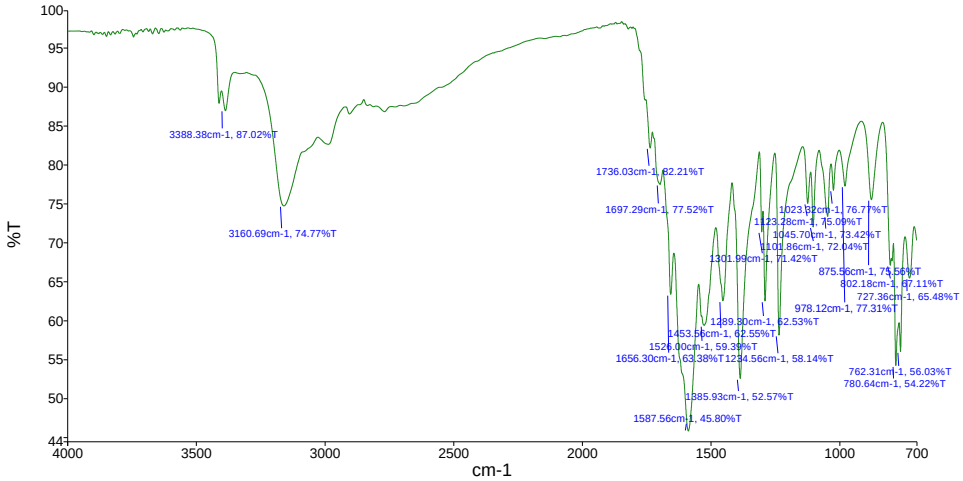

Figure 46: IR spectra for compound 2m

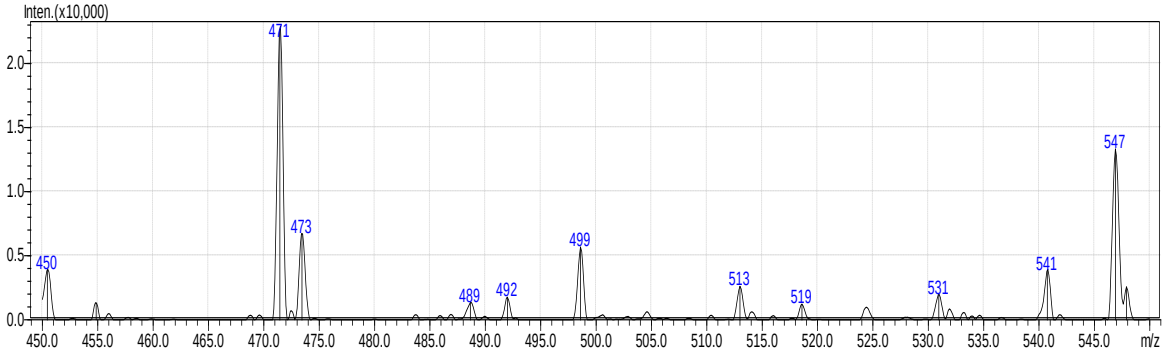

Figure 47: Mass spectra for compound 2m

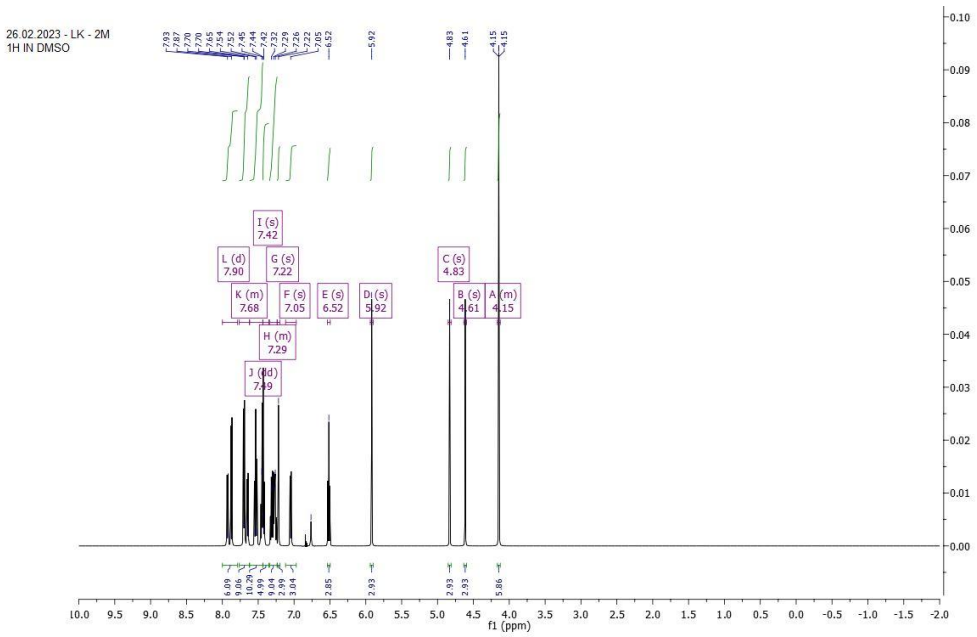

Figure 48: ^{1}H NMR for compound 2m

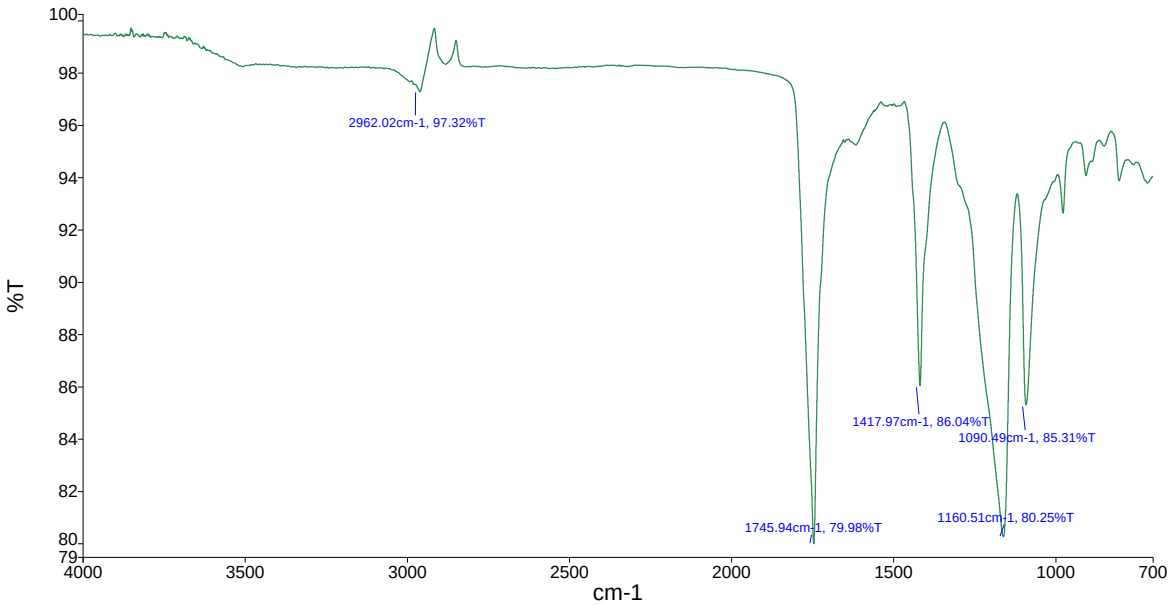

Figure 49: IR spectra for compound 3g

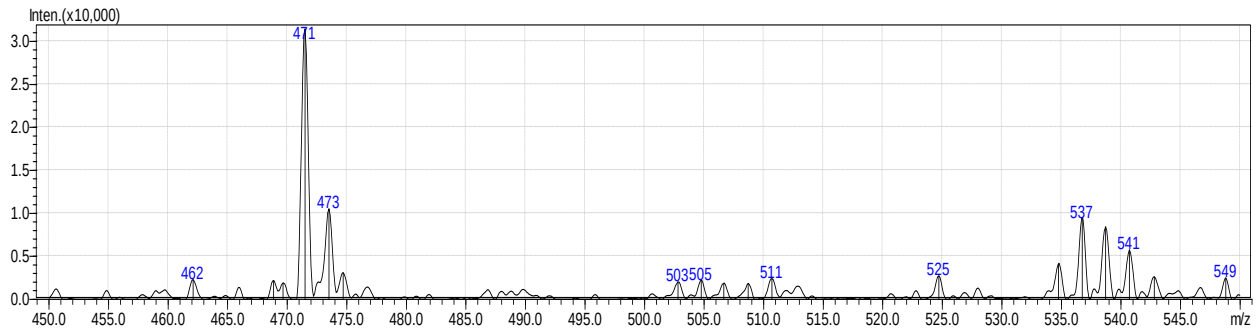

Figure 50: Mass spectra for compound 3g

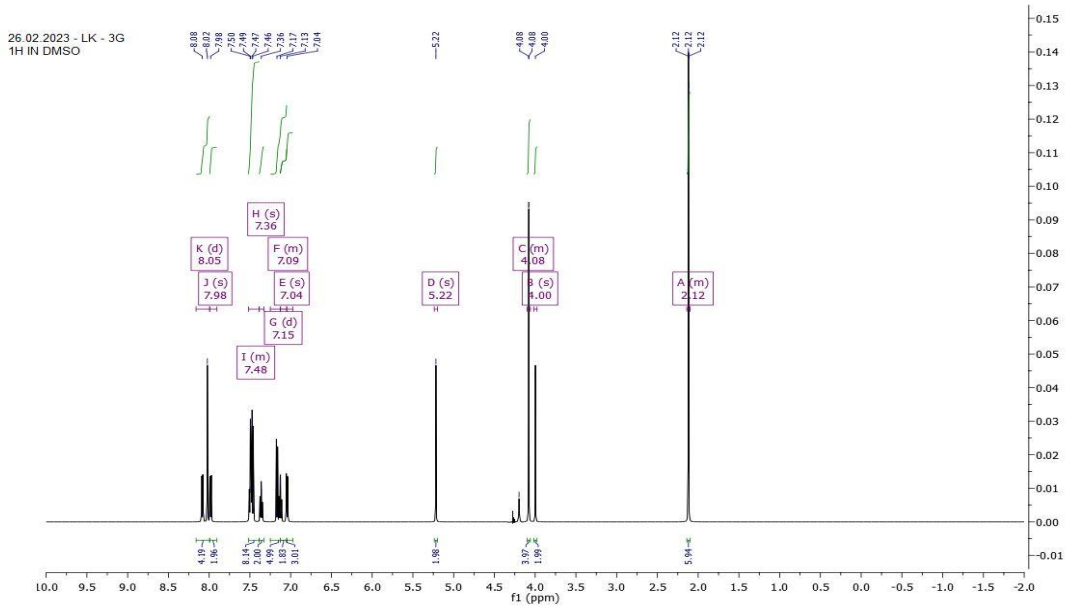

Figure 51: ^{1}H NMR for compound 3g

Figure 52: IR spectra for compound 3h

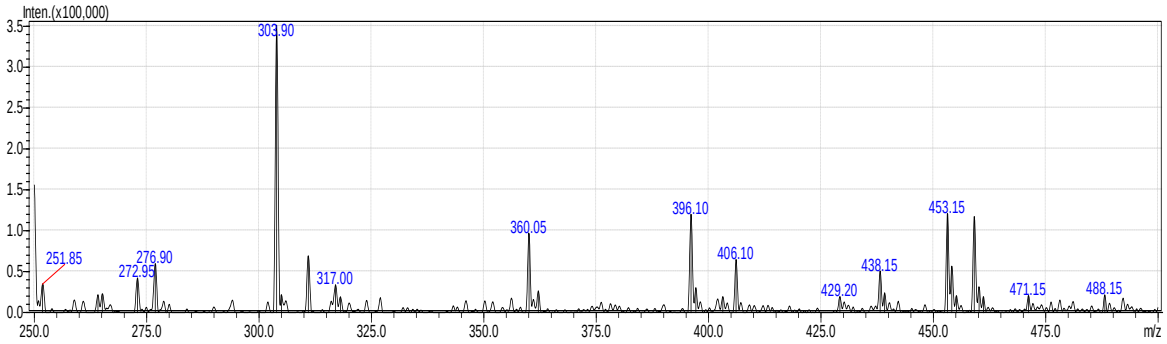

Figure 53: Mass spectra for compound 3h

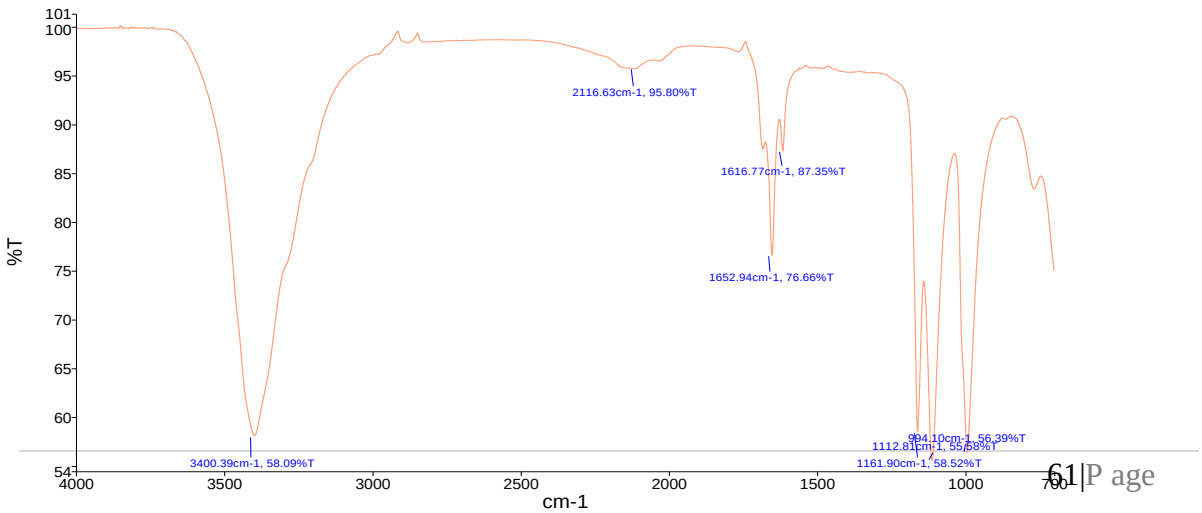

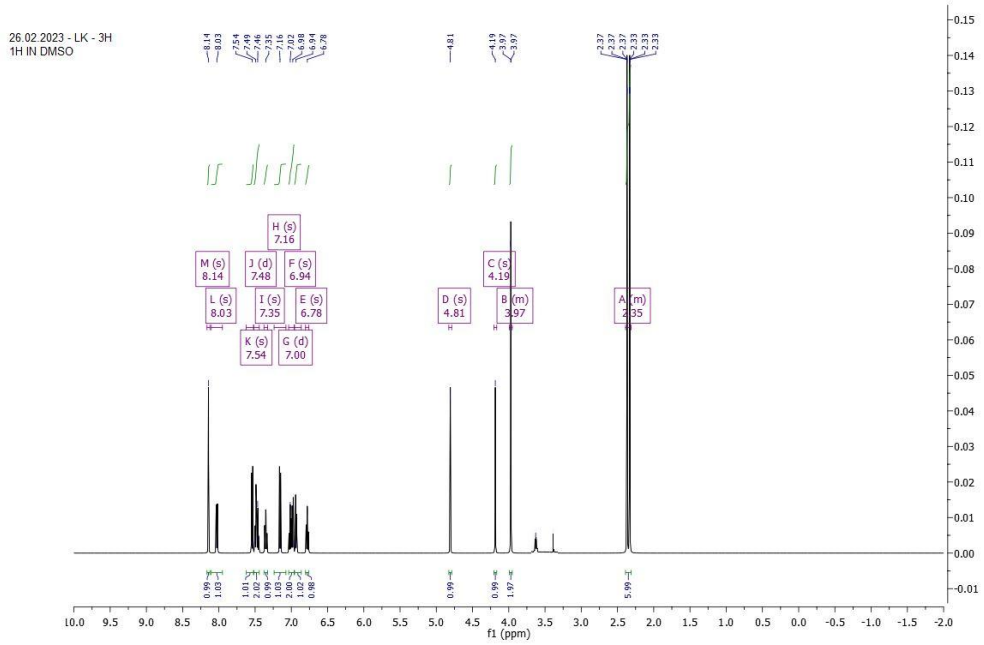

Figure54: ^{1}H NMR for compound 3h

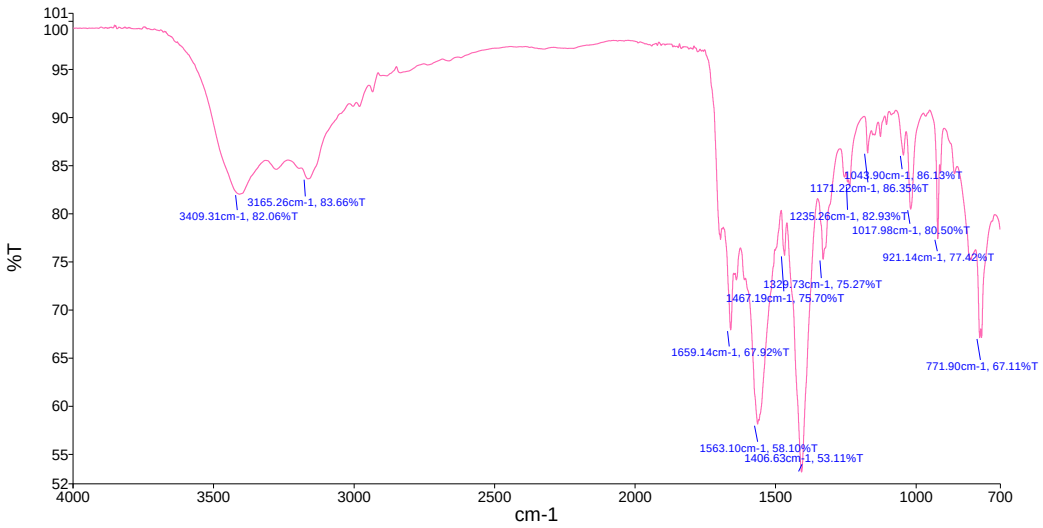

Figure 55: IR spectra for compound 3j

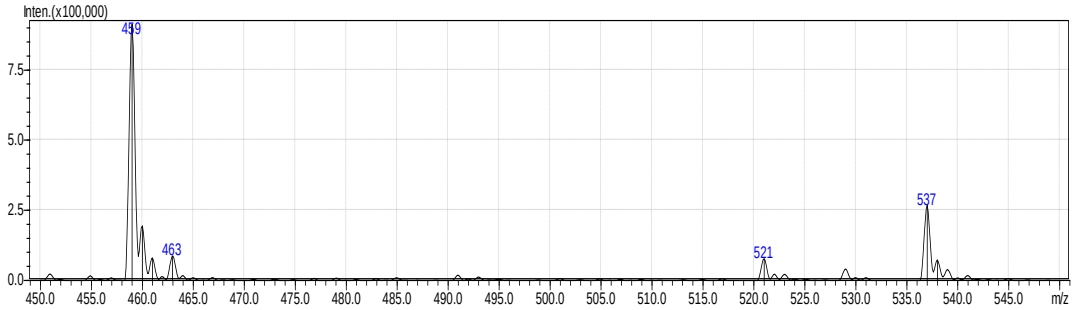

Figure 56: Mass spectra for compound 3j

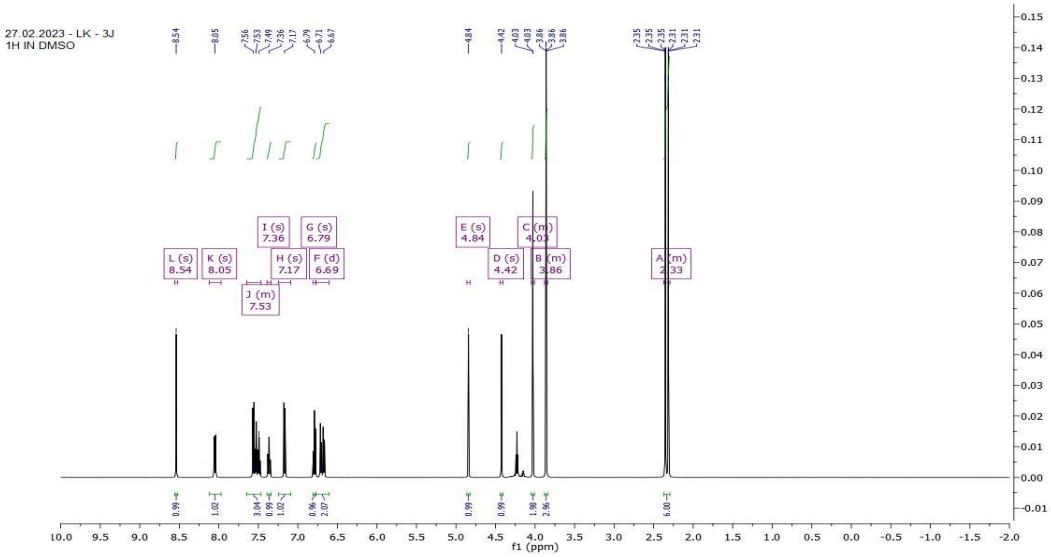

Figure 57: ^{1}H NMR for compound 3j

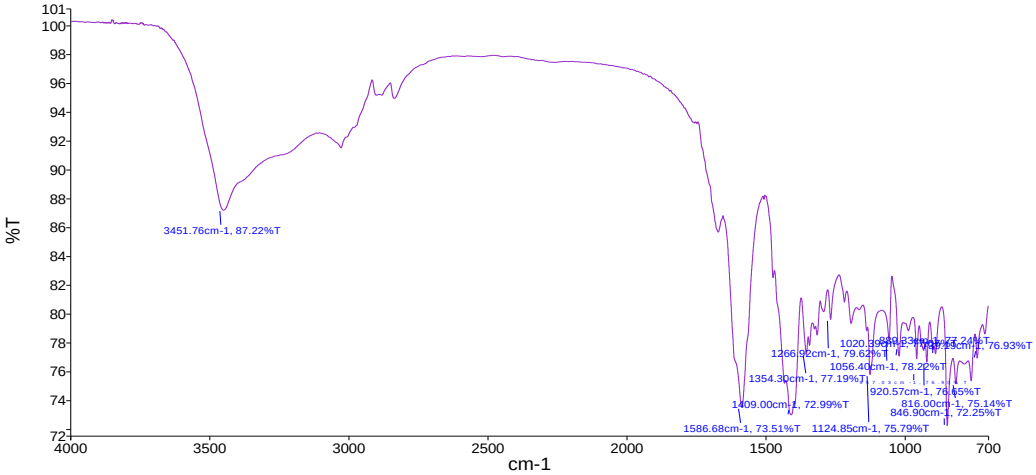

Figure 59: IR spectra for compound 3k

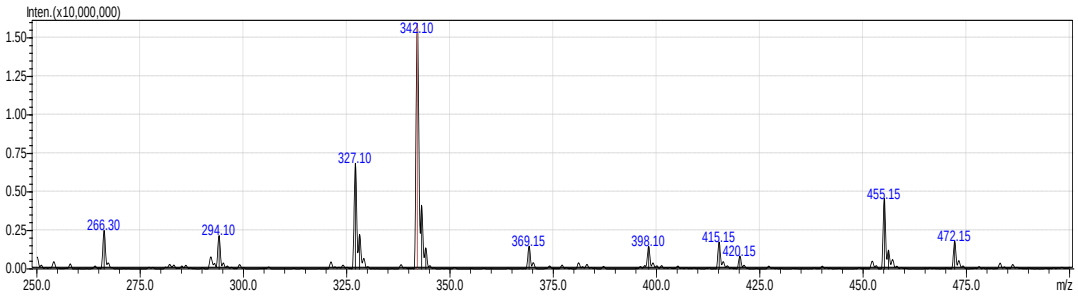

Figure 60: Mass spectra for compound 3k

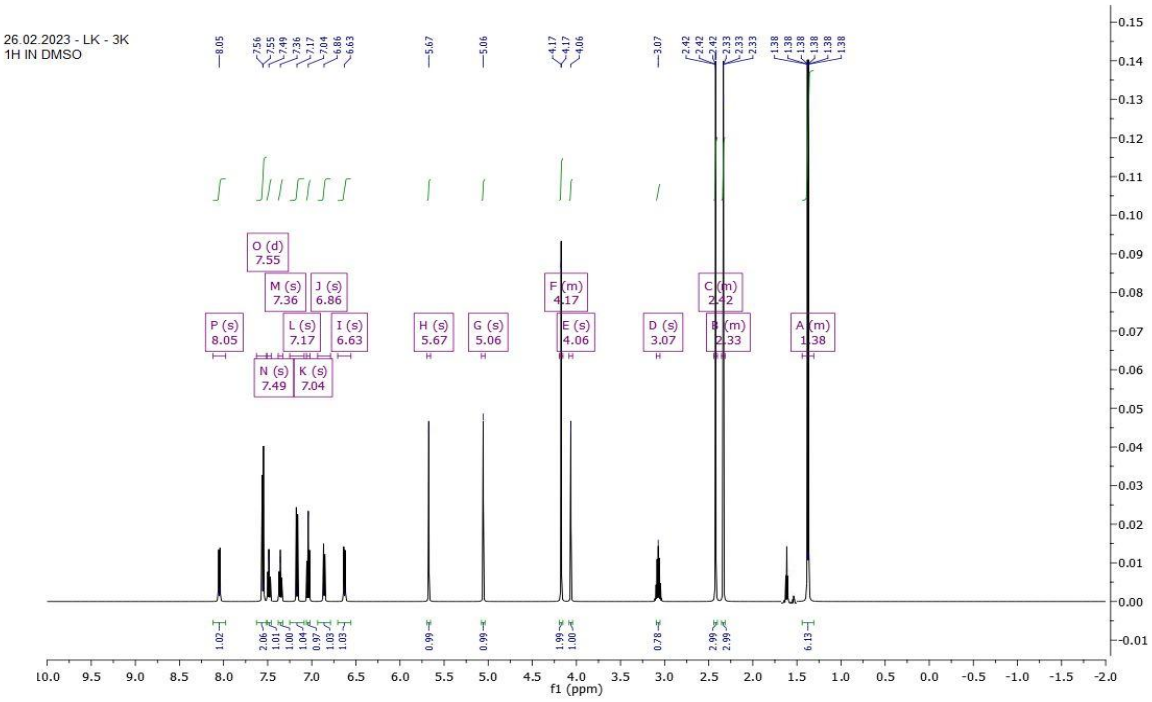

Figure 61:^{1}H NMR for compound 3k

6.5. *In-vitro* anticancer activity

Results of anticancer activity of the compounds were expressed as IC_{50} values which were determined by plotting the percentage cell viability versus concentration of sample on a logarithmic graph and reading off the control. The experiments were performed in triplicates, and then, the final IC_{50} values were calculated by taking average of triplicate experimental results. The results of in-vitro anti-cancer activity expressed in IC_{50} (µg/mL) are expressed in **table 2** and were compared to Daxorubicin. All 10 compounds are subjected to *in-vitro* cytotoxicity study by SRB assay method with cell lines MDA-MB-231 cell lines. All the tested compounds displayed an IC_{50}> 115 µg/mL at a concentration range of 30–250 µg/mL. Among the tested compounds, derivative 1f substituted with chlorobenzne shows a significant IC_{50}value (76.23 µg/ml) and fallowed by compound 2m substituted with furan derivative (78.43 µg/ml) shows good inhibition in breast cancer cell line. Remaining all other tested compounds shows good to moderate cytotoxic activity on tested cell line.

Table 4. Date for *invitro* cell line study

Sl No	Compound code	MDA-MB-231 (IC_{50}µg/ml)
1	1d	114.16
2	1f	76.23
3	1m	96.54
4	2l	89.92
5	2k	123.39

6	2m	78.34
7	3g	88.27
8	3h	85.32
9	3j	114.16
9	Olaparib	10.14
10	Niclosamide	12.52

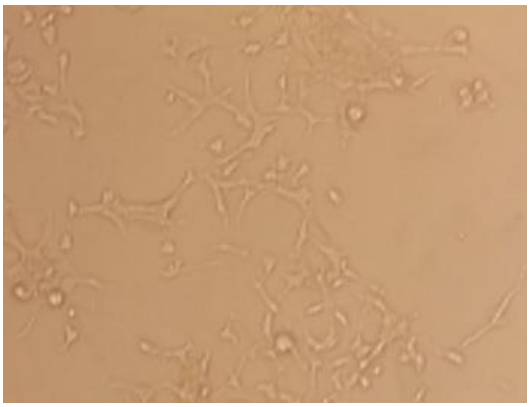

1d

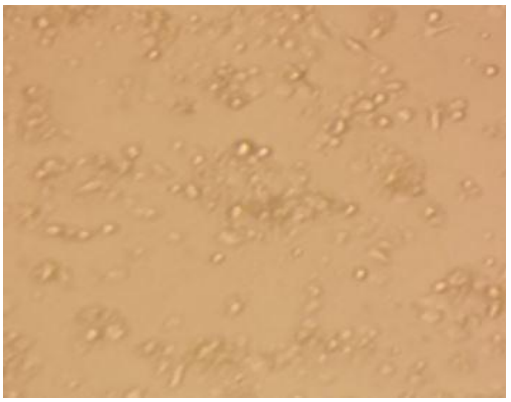

1f

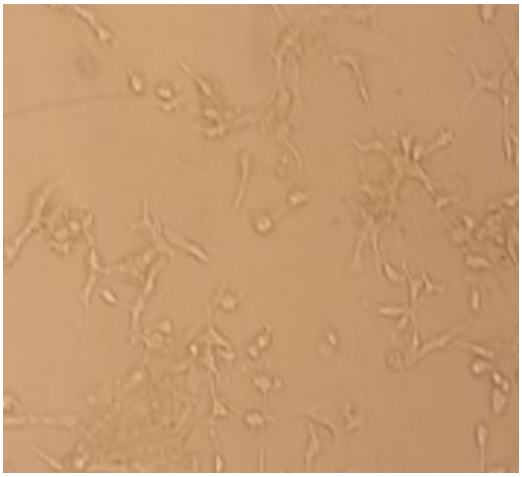

1m

2l

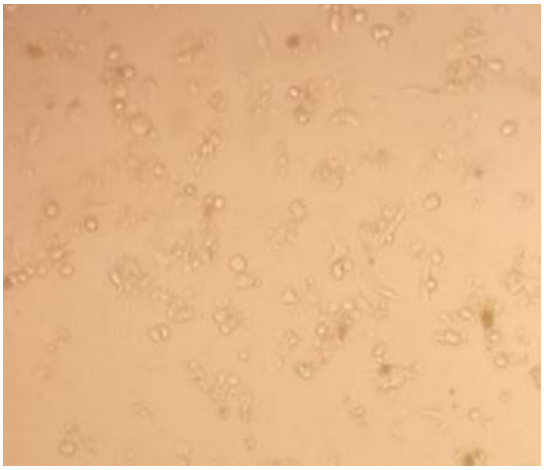

2k

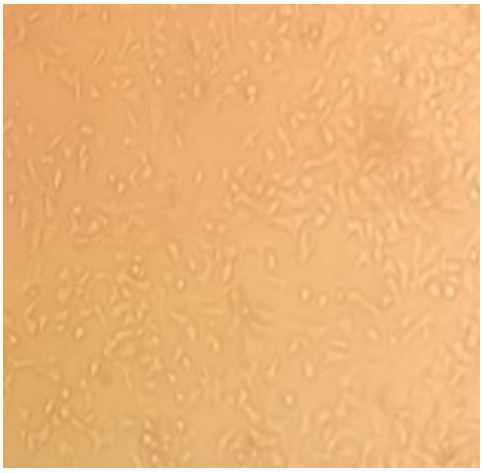

2m

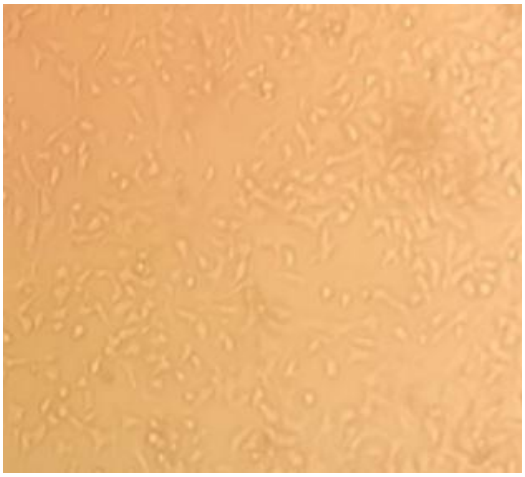

3g

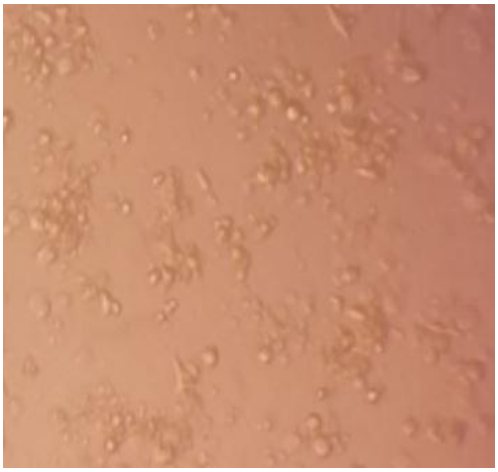

3h

Figure 62. Results of anticancer activity of the compounds

7. SUMMARY AND CONCLUSION

Summary

The synthesis of titled compounds was achieved by following synthetic routes as shown in the scheme. The synthesis of title compounds was achieved in good yield by simple techniques. It was chemically stable and available in good yield. The sharp melting point and unique spot-on TLC indicated that title compounds were obtained in pure form. The synthesized Compounds were purified by successive recrystallization from the appropriate solvents. These compounds also exhibited appropriate peaks at corresponding δ ppm in their ^{1}H-NMR spectra and corresponding molecular ion peaks in LC-MS spectra which conformed with the assigned structures. The interpretation of IR, ^{1}H NMR, and LC-MS spectra confirmed the structure of the title compounds.

All the designed compounds were subjected to molecular docking studies using Schrodinger's suite software. All the studied compounds show the significant docking score and which is compared with standard drug Olaparib and niclosamide. All the synthesized compounds were subjected to in vitro anti-cancer activity by SRB assay using MDA-MD-231 cell line studies.

Conclusion

It could be concluded from the present investigation that the benzimidazole derivative possess the most potent anticancer molecules.

REFERENCES

1. MahinG,HamedK.RoleofBiotechnologyinCancerControl.*Int.J.*Sci.Res.2015; 5:180–*18*5.
2. AaronJS,JohnO,DinoPrato.ImmunotherapyinCancerTreatment.OpenJ.Med . Microbiol.2014;4:178-191.
3. AkulapalliS.HistoryofCancer,AncientandModernTreatmentMethods.J.CancerSci. Ther.2009;1(2):1948–5956.
4. Yapeng,H,LiwuF.Targetingcancerstemcells:anewtherapytocurecancerpatients.Am.J. CancerRes.2012;2(3):340-356.
5. AnantNB,RohitM,AbdullahF,AmitV,DwarakanathBS.Cancerbiomarkers-Currentperspectives.IndianJ.Med.Res. 2010;132:129-149.
6. Milena J, Aleksandar A, Jelena P, Nevena G, Jelena M, Marija M, Jelena P,Tibor S, Danilo V, Gordana DR, Nebojsa A. The organic ester O,O'-diethyl-(S,S)-ethylenediamine-N,N'-di- 2-(3-cyclohexyl)propanoate dihydrochlorideattenuatesmurinebreastcancergrowthandmetastasis.Oncotarget.2018;9(46):28195–28212.
7. Marie FL, Jamie LP, Swati R, John MP. Crystal Structures of Poly(ADP-ribose) Polymerase-1 (PARP-1) Zinc Fingers Bound to DNA. J. Biochem.2011;286(12):10690 –10701.
8. Tobias K, Martin H, Patrick S, Linda S, Herwig S. Crystal Structure of theCatalytic Domain of Human PARP2 in Complex with PARP Inhibitor ABT-888.Biochemistry.2010;49:1056–1058.
9. Albert AA, Andrea C, Roberto N, Aydie H, Emidio C, Jordi M, Roberto P,Antonio M. Exploring the effect of PARP-1 flexibility in docking studies. J.Mol.Graph. Model.2013;45:192– 201.
10. DarnellJE.STATsandgeneregulation.Science.2000;277:1630-1635.
11. Levy DE, Darnell J. STATs transcriptional control and biologic impact. Nat.Rev.Mol. Cell. Biol.2002;3:651-662.
12. AilianX,ZhengduoY,YichengS,JiaZ,QiangS.TranscriptionfactorSTAT3asanovelmoleculartargetforcancerprevention.Cancers.2014;6:926-957
13. Michelle AB, Jiazhi S, Alan C, James T, Richard J, Saıd MS. Discovery ofJSI-124 (Cucurbitacin I), a selective Janus Kinase/Signal Transducer

andActivator of Transcription 3 signaling pathway inhibitor with potent antitumoractivity against human and murine cancer cells in mice. Cancer Res. 2003;63:1270–1279.

14. Florian MC, Carina O, Richard M, Svetlana AT, Stefan W, Edith BP, DanielaB, Roland K, Lukas AH, Kurt Z, Hartmut B, Peter O, Alexander S, Karl JH,Karlheinz F. Persistent STAT3 activation in colon cancer is associated withenhanced cell proliferation and tumor growth. Neoplasia. 2005;7(6):545 –555.
15. OBoyleNM,MeeganMJ.Designedmultipleligandsforcancertherapy.Curr.Med.Chem. 2011**;**18:4722-4737.
16. AnighoroA,BajorathJ,RastelliG.Polypharmacology:Challengesandopportunitiesindrugdiscovery.J.Med.Chem.2014**;***57*:7874-7887.
17. Costantino L, Barlocco D. Designed multiple ligands: Basic research vsclinicaloutcomes.Curr. Med.Chem.2012**;**19:3353-3387.
18. Roko Z, Andreja M, Eva B, Ivan A. Molecular insights into poly(ADP-ribose)recognitionandprocessing.Biomolecules*.*2013;3:1-17.
19. Julio CM, Longshan, L, Farjana JF, Ying D, Erik AB, Malina P, Jinming G,David AB. Review of poly (adp-ribose) polymerase (PARP) mechanisms ofaction and rationale for targeting in cancer and other diseases.CriticalReviewsTMinEukaryotic. GeneExpr. 2014;24(1):15-28.
20. HongyanL,AntoinetteRT.PARPinhibitors.*Curr.BreastCancerRep*.2011;3:44–54.
21. Turkson J, Bowman T, Garcia R, Caldenhoven E, De Groot RP, Jove R.STAT3 activation by Src induces specific gene regulation and is required forcelltransformation.Mol. Cell.Biol.1998;18(5):2545–2552.
22. SuiqingC,MinZ,LirongC.OverexpressionofphosphorylatedSTAT3correlated with the invasion andmetastasis of cutaneoussquamouscellcarcinoma. J.Dermatol.2005;32(5):354–360.
23. Qiu Z, Huang C, Sun J. RNA interference-mediated signal transducers andactivators of transcription 3 gene silencing inhibits invasion and metastasisofhumanpancreaticcancercells.CancerSci. 2007;98(7):1099–1106.
24. Martic S, Rains MK, Haftchenary S, Shahani VM, Kraskouskaya D, Ball DP,GunningPT,KraatzHB.ElectrochemicaldetectionoftheFc-

STAT3phosphorylationandSTAT3–Fc-STAT3dimerizationandinhibition.Mol.Bio.Syst. 2014;10:576.

25. Jochen S, Bianca S, Angela H, Thomas UM, Thorsten B. Stattic: a small-moleculeinhibitorofSTAT3activationanddimerization.Chem.Biol.2006;13:1235–1242.
26. Omar NL, Fredrick JB, Xiaofu W, Na Y, Tiziana C, Yesenia RK, Haijun C,Haiying C, Jia Z, Ravi SR. STAT3 inhibition suppresses hepatic stellate cellfibrogenesis: HJC0123, a potential therapeutic agent for liver fibrosis. RSCAdv. 2016;6:100652–100663.
27. Nan C, Wei Z, Lan LY, Jun C, Qiu NL, Gang C, Jia JC. The STAT3 inhibitorpimozide impedes cell proliferation and induces ROS generation in humanosteosarcoma bysuppressingcatalaseexpression.Am. J.Transl.Res.2017;9(8):3853-3866.
28. Lim R, Ahmed N, Borregaard N, *et al.* Neutrophil gelatinase associatedlipocalin (NGAL) an early-screening biomarker for ovarian cancer: NGAL isassociatedwithepidermalgrowthfactorinducedepithelio-mesenchymaltransition.Int. J. Cancer. 2007;120(11):2426-34.
29. ChenL,WangJ,WuJ,ZhengQ,HuJ.Indirubinsuppressesovariancancercell viabilities through the STAT3 signaling pathway. Drug Des. Devel. Ther.2018;12:3335-42.
30. Chaluvally RP, Jeong KJ, Pradeep S, *et al.* Direct upregulation of STAT3 bymicrorna-551b-3pderegulatesgrowthandmetastasisofovariancancer.CellRep.2016;15(7):1493-504.
31. Zhong LX, Li H, Wu ML, *et al.* Inhibition of STAT3 signaling as criticalmolecular event in resveratrol-suppressed ovarian cancer cells. J. OvarianRes.2015;8:25.
32. Park E, Park J, Han SW, Im SA, Kim TY, Oh DY, Bang YJ. NVP-BKM120, anovel PI3K inhibitor, shows synergism with a STAT3 inhibitor in humangastriccancercellsharboringKRASmutations.Int.J.Oncol.2011;40(4):1259-66.
33. Zeng H, Zhang H, Jang F, Zhao L, Zhang J. Molecular modelling studies onbenzimidazolecarboxamidederivativesasPARP-1inhibitorsUsing3D-QSARanddocking.Chem. Biol.Drug Des.2011;78:333–352.

34. Ye N, Chen CH, Chen TT, Song Z, He JX, Huan XJ, Song SS, Liu Q, ChenY, Ding J, Xu Y,Miao ZH, Zhang A. Design, Synthesis and BiologicalEvaluation of a Series of Benzo[de][1,7]naphthyridin-7(8H)-ones bearing afunctionalized longer chain appendage as novel PARP1 Inhibitors. J. Med.Chem.2013;4:134-149.
35. Amini KM, Anwar MM, Kamil MM, Kaseem EMM, Syam YM, Elseginy SA.Synthesis,cytotoxicevaluationandmoleculardockingstudyofnovelquinazolinederivativesasPARP-1inhibitors.ActaPol.Pharm.2013;70(5):833–849.
36. DeepakC,KarthikeyanC,ChoureL,SiddiquiS,GuptaM,ArshadM,TrivediP. Synthesis, characterization and anti-cancer activity of some fluorinated3,6-diaryl-[1,2,4]triazolo[3,4-b][1,3,4]thiadiazoles.Arab.J.Chem.2013;5:843 –859.
37. ZhangX,MingboS,ChenY,LiJ,LuW.TheDesignandSynthesisofaNewClass of RTK/HDACDual-Targeted Inhibitors. Molecules, 2013;18:6491-6503.
38. Nan J, Du Y, Chen X, Bai Q, Wang Y, Zhang X, Zhu N, Zhang J, Hou J, QinWang, Yang J. TPCA-1 Is a direct dual inhibitor of STAT3 and nf-kb andregresses mutant EGFR-associated human non–small cell lung Cancers.Mol.Cancer Ther. 2014;13(3):617–29.
39. Daka P, Aiguo L, Chamini K, Erika C, Cameron W, Hui X, Jiay U, ZhenghuX,RichardC.Design,synthesisandevaluationofXZH-5analogueasSTAT3inhibitors.Bioorg.Med. Chem.2015;23(6):1348-1355.
40. Patel MR, Bhatt A, Steffen JD, Chergui A, Murai J, Pommier Y, Pascal JM,Trombetta LD, Fronczek FR, Talele TT. Discovery and structure−activityrelationshipofnovel2,3-dihydrobenzofuran-7-carboxamideand2,3-dihydrobenzofuran-3(2h)-one-7-carboxamidederivativesaspoly(adpribose)polymerase-1inhibitors.J.Med.Chem.2014;57(13):5579–5601.
41. Wang L, Feng L, Ning J, Wenxia Z, Xinbo Z, Zhibing Z. Design, synthesis,andbiologicalevaluationofnovelparp-1inhibitorsbasedona1h-thieno[3,4-d]imidazole-4-carboxamide scaffold.Molecules.2016;21:772–787
42. YangEG,MustafaN,TanEC,PoulsenA,RamanujuluPM,ChngWJ,JeffreyJ, Yen JY, Dymock BW.Design and synthesis of janus kinase 2 (jak2) andhistone deacetlyase (HDAC) bispecific inhibitors based on pacritinib andevidenceofdualpathwayinhibitioninhematologicalcelllines.J.Med.Chem. 2016;59(18):8233-62.